

# Target Detection and Tracking in a Pulse Doppler Radar



By

PC Altamash Ahmed

Capt Usman Firdous

PC Nauman Hamid

GC Syed Bilal Haider

Submitted to Faculty of Electrical Engineering  
National University of Science and Technology, Rawalpindi  
in partial fulfillment for the requirements of a B.E. Degree in  
Telecommunication Engineering.

April 2006

# List of Figures

- **Figure 1.1 Basic Principle of Radar** ..... page 2
- **Figure 1.2 Range and velocity of target w.r.t. radar** ..... page 4
- **Figure 1.3. CW radar block diagram.** ..... page 6
- **Figure 1.4 Amplitude Spectrum for a continuous sine wave** ..... page 7
- **Figure 1.5 Block diagram of pulse Doppler radar** ..... page 7
- **Figure 2.1 Simple CW and Pulse Doppler radar block diagram** ..... page 14
- **Figure 3.1 Geometry of radar and target in deriving the Doppler frequency shift** ... page 19
- **Figure 3.2 Different Target's Doppler Shift** ..... page 20
- **Figure3.3. Train of transmitted and received pulses** ..... page 21
- **Figure 3.4. Radar Geometry of radar surface clutter** ..... page 22
- **Figure3.5 Representation of the echo pulse train** ..... page 25
- **Figure4.1 Received Waveform** ..... page 27
- **Figure 4.2 I ,Q Demodulation** ..... page 30
- **Figure 4.3 Single Delay Line canceller** ..... page 33
- **Figure 4.4 Two configurations for a double delay line canceller** ..... page 34
- **Figure 4.5 Normalized frequency responses for single and double cancellers** .... page35
- **Figure 5.1 Simplified block diagram of TWS data processing** ..... page38
- **Figure 5.2 an implementation for a  $\alpha\beta$  tracker** ..... page 40
- **Figure 5.3 an implementation for a  $\alpha\beta\gamma$  tracker** ..... page 41
- **Figure 6.1 I/Q Demodulator** ..... page 43
- **Figure 6.2 Transmitted Signal at IF stage** ..... page 43
- **Figure 6.3 Target Return** ..... page 44

- **Figure 6.4 Clutter Return** ..... page 44
- **Figure 6.5 Impulse Response of LPF** ..... page 45
- **Figure 6.6 Frequency Response of LPF** ..... page 46
- **Figure 6.7 Filtered & down sampled I channel Output for target** ..... page 47
- **Figure 6.8 Filtered & down sampled Q channel Output for target** ..... page 47
- **Figure 6.9 Filtered & down sampled I channel Output for clutter** ..... page 48
- **Figure 6.10 Filtered & Down sampled Q channel Output for clutter** ..... page 48
- **Figure 6.11 Simulated radar base band data** ..... page 49
- **Figure 6.12 Output of DLC when clutter was not decorrelating** ..... page 50
- **Figure 6.13 Output of Adaptive Filter when clutter was not decorrelating** ..... page 51
- **Figure 6.14 Output of DLC when clutter was decorrelating** ..... page 52
- **Figure 6.15 Output of Adaptive Filter when clutter was decorrelating** ..... page 53
- **Figure 6.15 Block diagram of a CA-CFAR processor** ..... page 54
- **Figure 6.16 Output after application of CA-SO-CFAR algorithm** ..... page 55
- **Figure 6.17 Output after application of CA-GO-CFAR algorithm** ..... page 56
- **Figure 6.18 Output after application of CA-AVE-CFAR algorithm** ..... page 57
- **Figure 6.19 Output after application of OS-CFAR algorithm** ..... page 58
- **Figure 6.20 MLE-CFAR processor** ..... page 59
- **Figure 6.21 Output after application of MLE-CFAR algorithm** ..... page 60
- **Figure 6.22 Output of FFT of the four targets** ..... page 61
- **Figure 6.23 MEM Output** ..... page 62
- **Figure 6.24 PPI Display of targets being tracked** ..... page 63
- **Figure 6.25 Outputs alpha-beta and alpha-beta-gamma tracker for target no.1** ..... page 64

- **Figure 6.26 Outputs alpha-beta and alpha-beta-gamma tracker for target no.2 . . . . . page 64**
- **Figure 6.27 Outputs alpha-beta and alpha-beta-gamma tracker for target no.3 . . . . . page 65**
- **Figure 6.28 Actual Radar Signal . . . . . page 66**
- **Figure 6.29 Actual Radar Signal after adaptive clutter filtering . . . . . page 67**
- **Figure 6.29 Threshold radar signal . . . . . page 68**
- **Figure 6.30 Spectral Estimate of the threshold signal . . . . . page 69**

# Chapter 1

## INTRODUCTION

The term radar is a contraction of the words radio detection and ranging. Radar is an electromagnetic system for the detection and location of reflecting objects such as aircraft, ships, spacecraft, vehicles, people, and the natural environment. It operates by radiating energy into space and detecting the echo signal reflected from an object, or target. The reflected energy that is returned to the radar not only indicates the presence of a target, but by comparing the received echo signal with the signal that was transmitted its location can be determined along with other target-related information.

The basic principle of radar is illustrated in Figure down below. A transmitter (in the upper left portion of the figure) generates an electromagnetic signal (such as a short pulse of sine wave) that is radiated into space by an antenna. A portion of the transmitted energy is intercepted by the target and reradiated in many directions. The radiation directed back towards the radar is collected by the radar antenna, which delivers it to a receiver. There it is processed to detect the presence of the target and determine *its* location. A single antenna is usually used on a time-shared basis for both transmitting and receiving when the radar waveform is a repetitive series of pulses. The range, or distance, to a target is found by measuring the time it takes for the radar signal to travel to the target and return back to the radar. (We use the term *range* to mean *distance*, which is not the definition of range found in some dictionaries. The target's location in angle can be found from the direction the narrow beam width radar antenna points when the received echo signal is of maximum amplitude. If the target is in motion, there is a shift in the frequency of the echo signal due to the Doppler effect. This frequency shift is proportional to the velocity of the target relative to the radar (also called the radial velocity). The Doppler frequency shift is widely used in radar as the basis for separating desired moving targets from fixed (unwanted) "clutter" echoes reflected from the natural environment such as land, sea, or rain. Radar can also provide information about the nature of the target being observed. [1]

## 1.2 Range to a Target

The most common radar signal, or waveform, is a series of short duration, somewhat rectangular-shaped pulses modulating a sine wave carrier. (This is sometimes called a *pulse train*.) The range to a target is determined by the time  $T_R$  it takes the radar signal to travel to the target and back. Electromagnetic energy in free space travels with the speed of light, which is  $c = 3 \times 10^8 \text{ m/s}$ . Thus the time for the signal to travel to a target located at a range  $R$  and return back to the radar is  $2R/c$ . The range to a target is then

$$R = cT_R/2 \quad [1.1]$$

With the range in kilometers or in nautical miles, and  $T$  in microseconds, Eq. (1.1) becomes.

$$R \text{ (km)} = 0.15 T_R \text{ (\mu s)} \quad \text{or} \quad R \text{ (nmi)} = 0.081 T_R \text{ (\mu s)}$$

Each microsecond of round-trip travel time corresponds to a distance of 150 meters, 164 yards, 492 feet, 0.081 nautical miles, or 0.093 statute mile. It takes 12.35  $\mu\text{s}$  for a radar signal to travel a nautical mile and back.

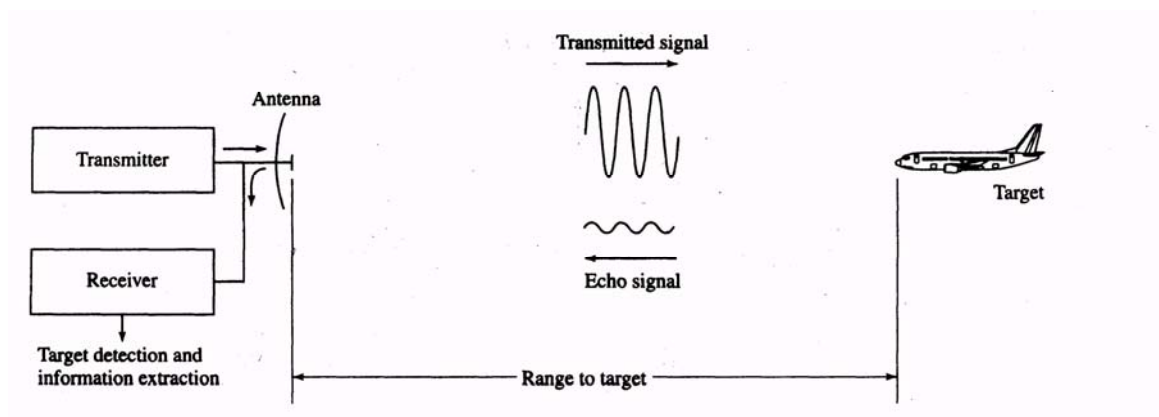


Figure 1.1 Basic Principle of Radar [1]

## 1.3 Maximum Unambiguous Range

Once a signal is radiated into space by radar, sufficient time must elapse to allow all echo signals to return to the radar before the next pulse is transmitted. The rate at which pulses may be transmitted, therefore, is determined by the longest range at which targets are expected. If the time between pulses  $T_p$  is too short, an echo signal from a long-range target might arrive after the transmission of the next pulse and be mistakenly associated with that pulse rather than the actual pulse transmitted earlier. This can result in an incorrect or ambiguous measurement of the range. Echoes that arrive after the transmission of the next pulse are called *second-time-around echoes* (or *multiple-time-around echoes* if from even earlier pulses). Such an echo would appear to be at a closer range than actual and its range measurement could be misleading if it were not known to be a second-time-around echo. The range beyond which targets appear as second-time-around echoes is the *maximum unambiguous range*,  $R_{un}$ , and is given by

$$R_{un} = cT_p/2 = c/2f_p$$

Where  $T_p$  = pulse repetition period =  $1/f_p$ , and  $f_p$  = pulse repetition frequency (prf), usually given in hertz or pulses per second (pps).

## 1.4 Doppler Frequency Shift

The doppler effect used in radar is the same phenomenon that was introduced in high school physics courses to describe the changing pitch of an audible siren from emergency vehicle as it travels toward or away from the listener. Here we are interested in the doppler effect that changes the frequency of the electromagnetic signal that propagates from the radar to a moving target and back to the radar. If the range to the target is  $R$ , then the total number of wavelengths  $\lambda$  in the two-way path from radar to target and return is  $2R/\lambda$ . Each wavelength corresponds to a phase change of  $2\pi$  radians. The total phase change in the two-way propagation path is then

$$\Phi = 2\pi \times 2R / \lambda = 4\pi R / \lambda \quad [1.2]$$

If the target is in motion relative to the radar,  $R$  is changing and so will the phase. Differentiating Eq. (1.2) with respect to time gives the rate of change of phase, which is angular frequency [2]

$$\omega_d = \frac{d\Phi}{dt} = \frac{4\pi}{\lambda} \frac{dR}{dt} = \frac{4\pi v_r}{\lambda} = 2\pi f_d \quad [1.3]$$

where  $v_r = dR/dt$  is the radial velocity (meters/second), or rate of change of range with time. If, as in Fig. 1.2, the angle between the target's velocity vector and the radar line of sight to the target is  $\theta$ , then  $v_r = v \cos \theta$ , where  $v$  is the speed, or magnitude of the vector velocity. The rate of change of  $\Phi$  with time is the angular frequency  $\omega_d = 2\pi f_d$

where  $f_d$  is the *doppler frequency shift*. Thus from Eq. (1.3),

$$f_d = \frac{2v_r}{\lambda} = \frac{2f_r v_r}{c} \quad [1.4]$$

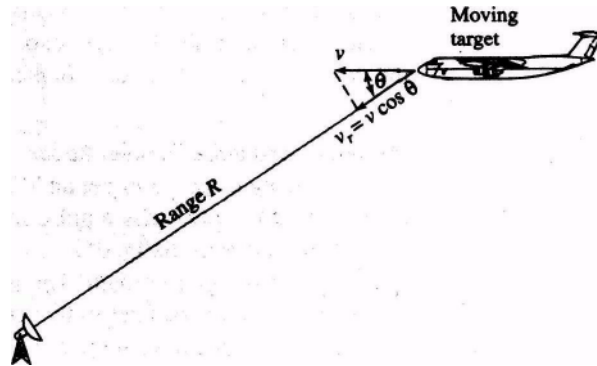


Figure 1.2 Range and velocity of target w.r.t. radar [1]



## 1.5 RADAR TYPES

### 1.5.1 Continuous Wave (CW) radars

Continuous Wave (CW) radars utilize CW waveforms, which may be considered to be a pure sine wave of the form  $\cos 2\pi f_o t$ . Spectra of the radar echo from stationary targets and clutter will be concentrated at  $f_o$ . The center frequency for the echoes from moving targets will be shifted by  $f_d$ , the Doppler frequency. Thus by measuring this frequency difference CW radar can very accurately extract target radial velocity. Because of the continuous nature of CW emission, range measurement is not possible without some modifications to the radar operations and waveforms.

In order to avoid interruption of the continuous radar energy emission, two antennas are used in CW radars, one for transmission and one for reception. Fig.1.3 shows a simplified CW radar block diagram. The appropriate values of the signal frequency at different locations are noted on the diagram. The individual Narrow Band Filters (NBF) must be as narrow as possible in bandwidth in order to allow accurate Doppler measurements and minimize the amount of noise power.

In theory, the operating bandwidth of a CW radar is infinitesimal (since it corresponds to an infinite duration continuous sinewave). However, systems with infinitesimal bandwidths cannot physically exist, and thus the bandwidth of CW radars is assumed to correspond to that of a gated CW waveform. [1]

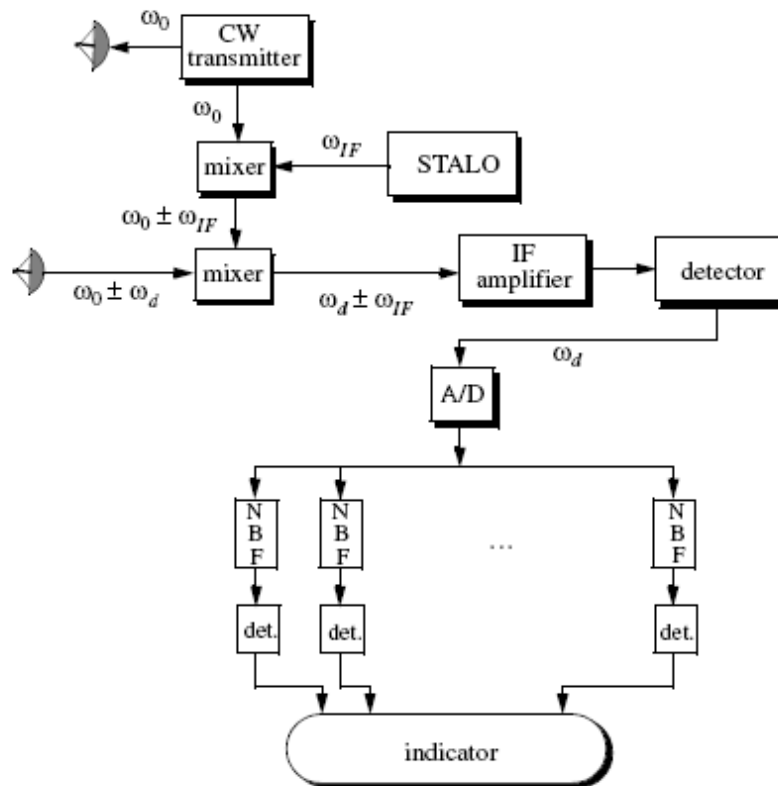


**Figure 1.3. CW radar block diagram.[1]**

The NBF bank (Doppler filter bank) can be implemented using a Fast Fourier Transform (FFT). If the Doppler filter bank is implemented using an FFT of size  $N$ , and if the individual NBF bandwidth (FFT bin) is  $\Delta f$ , then the effective radar Doppler bandwidth is  $N \Delta f$ . The reason for the one-half factor is to account for both negative and positive Doppler shifts. Since range is computed from the radar echoes by measuring a two-way time Delay, then single frequency CW radars cannot measure target range. In order for CW radars to be able to measure target range, the transmit and receive waveforms must have some sort of timing marks. By comparing the timing marks at transmit and receive, CW radars can extract target range.

The timing mark can be implemented by modulating the transmit waveform, and one commonly used technique is Linear Frequency Modulation (LFM). Before we discuss LFM signals, we will first introduce the CW radar equation and briefly address the general Frequency Modulated (FM) waveforms using sinusoidal modulating signals.

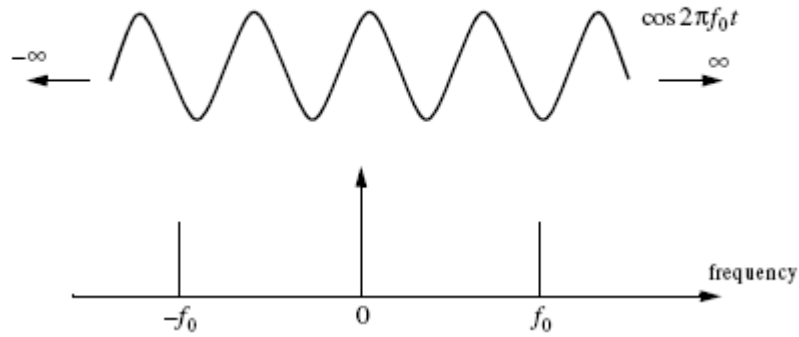


**Figure 1.4 Amplitude Spectrum for a continuous sine wave [1]**

### 1.5.2 Pulse Doppler radar

The radar frequency is  $f_t = c / \lambda$ , and the velocity of propagation  $c = 3 \times 10^8$  m/s. If the Doppler frequency is in hertz, the radial velocity in knots (abbreviated kt), and the radar wavelength in meters, we can write

$$f_d(\text{Hz}) = \frac{1.03 v_r(\text{kt})}{\lambda(\text{m})} = \frac{v_r(\text{kt})}{\lambda(\text{m})} \quad [1.5]$$

The doppler frequency in hertz can also be approximately expressed as  $3.43 v_r f_t$  where  $f_t$  is the radar frequency in GHz and  $v_r$  is in knots.

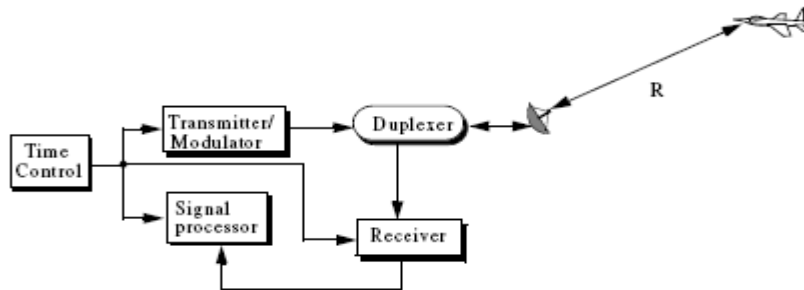


**Figure 1.5 Block diagram of pulse Doppler radar [3]**

## 1.6 RADAR FREQ BAND

Radar Frequency Bands		
Band Designation	Frequency Range	Typical Usage
VHF	50-330 MHz.	Very long-range surveillance
UHF	300-1,000 MHz.	Very long-range surveillance
L	1-2 GHz.	Long-range surveillance, enroute traffic control
S	2-4 GHz.	Moderate-range surveillance, terminal traffic control, long-range weather
C	4-8 GHz.	Long-range tracking, airborne weather
X	8-12 GHz.	Short-range tracking, missile guidance, mapping, marine radar, airborne intercept
K <sub>u</sub>	12-18 GHz.	High resolution mapping, satellite altimetry
K	18-27 GHz.	Little used (H <sub>2</sub> O absorption)
K <sub>a</sub>	27-40 GHz.	Very high resolution mapping, airport surveillance
mm	40-100+ GHz.	Experimental

**Table No.1 Radar Frequency Band [3]**

## 1.7 ORIGIN OF RADAR

The basic concept of radar was first demonstrated by the classical experiments conducted by the German physicist Heinrich Hertz from 1885 to 1888. Hertz experimentally verified the predictions of James Clerk Maxwell's theory of the electromagnetic field published in 1864. Hertz used an apparatus that was similar in

principle to pulse radar at frequencies in the vicinity of 455 MHz. He demonstrated that radio waves behaved the same as light except for the considerable difference in frequency between the two. He showed that radio waves could be reflected from metallic objects and refracted by a dielectric prism.

Hertz received quick and widespread recognition for his work, but he did not pursue its practical applications. This was left, to others. The potential of Hertz's work for the detection and location of reflecting objects—which is what radar does—was advanced by another German, Christian Hulsmeyer. In the early 1900s he assembled an instrument that would today be known as a monostatic (single site) pulse radar. It was much improved over the apparatus used by Hertz. In 1904 he obtained a patent in England and other countries. Hulsmeyer's radar detected ships, and he extensively marketed it for preventing collisions at sea. He demonstrated his apparatus to shipping companies and to the German Navy. Although it was a success and much publicized, there apparently was no interest for a ship collision-avoidance device. His invention and his demonstrations faded from memory and were all but forgotten. Radar would have to be rediscovered a few more times before it eventually became an operational reality.

During the 1920s other evidence of the radar method appeared. S. G. Marconi, the well-known pioneer of wireless radio, observed the radio detection of targets in his experiments and strongly urged its use in a speech delivered in 1922 before the Institute of Radio Engineers (now the IEEE)," Apparently unaware of Marconi's speech, A. Hoyt Taylor and Leo C. Young of the U.S. Naval Research Laboratory in Washington, D.C. accidentally observed, in the autumn of 1922, a fluctuating signal at their receiver when a ship passed between the receiver and transmitter located on opposite sides of a river. This was called a CW *wave-interference system*, but today it is known as *bistatic CW radar*. (*Bistatic* means the radar requires two widely separated sites for the transmitter and receiver.) In 1925, the pulse radar technique was used by Breit and Tuve of the Carnegie Institution in Washington, D.C. to measure the height of the ionosphere. The Breit and Tuve apparatus was indeed radar, but it was not recognized at the time that the same principle might be applied for the detection of ships and

aircraft. There were additional reported detections of aircraft and other targets by the CW wave-interference (bistatic radar) method in several countries of the world; but this type of radar did not have, and still doesn't have, significant utility for most applications.[3]

## 1.8 RADAR APPLICATION

Radar has been employed to detect targets on the ground, on the sea, in the air, in space, and even below ground. The major areas of radar application are briefly described below.

Military Radar is an important part of air-defense systems as well as the operation of Pensive missiles and other weapons. In air defense it performs the functions of surveillance and weapon control. Surveillance includes target detection, target recognition, target tracking, and designation to a weapon system. Weapon-control radars track targets, direct the weapon to an intercept, and assess the effectiveness of the engagement (called *battle damage assessment*). A missile system might employ radar methods for guidance and fuzing of the weapon. High-resolution imaging radars, such as synthetic aperture radar, have been used for reconnaissance purposes and for detecting fixed and moving targets on the battlefield. Many of the civilian applications of radar are also used by the military. The military has been the major user of radar and the major means by which new radar technology has been developed. Remote Sensing All radars are remote sensors; however, this term is used to imply the sensing of the environment. Four important examples of radar remote sensing are (1) weather observation, which is a regular part of TV weather reporting as well as a major input to national weather prediction; (2) planetary observation, such as the mapping of Venus beneath its visually opaque clouds; (3) short-range below-ground probing; and (4) mapping of sea ice to route shipping in an efficient manner.

Air Traffic Control (ATC) Radars have been employed around the world to safely control air traffic in the vicinity of airports (Air Surveillance Radar, or ASR), and en

route from one airport to another (Air Route Surveillance Radar, or ARSR) as well as ground-vehicular traffic and taxiing aircraft on the ground (Airport Surface Detection Equipment, or ASDE). The ASR also maps regions of rain so that aircraft can be directed around them. There are also radars specifically dedicated to observing weather (including the hazardous downburst) in the vicinity of airports, which are called Terminal Doppler Weather Radar, or TDWR. The Air Traffic Control Radar Beacon System (ATCRBS and Mode-S) widely used for the control of air traffic, although not a radar, originated from military IFF (Identification Friend or Foe) and uses radar-like technology.[3]

# Chapter 2

## RADAR WORKING

The simple form of the radar equation, expressed the maximum radar range  $R_{max}$  in terms of the key radar parameters and the target's radar cross section when the radar sensitivity was limited by receiver noise. It was written

$$R_{max} = \left[ \frac{P_t G A_e \sigma}{(4\pi)^2 S_{min}} \right]^{1/4} \quad [2.1]$$

where

- $P_t$  = transmitted power, W
  - $G$  = Antenna gain
  - $A_e$  = Antenna effective aperture, m<sup>2</sup>
  - $\sigma$  = Radar cross section of the target, m<sup>2</sup>
  - $S_{min}$  = Minimum detectable signal, W
- 

Except for the target's radar cross-section, the parameters of this simple form of the radar equation are under the control of the radar designer. It states that if long ranges are desired, the transmitted power should be large, the radiated energy should be concentrated into a narrow beam (large transmitting gain), the echo energy should be received by a large antenna aperture (also synonymous with large gain), and the receiver should be sensitive to weak signals.

### 2.1 RADAR INPUT SIGNAL

Radar input signal consist of following types of signals.

- Clutter returns
- Target echoes
- Noise



- EM interference

### **2.1.1 CLUTTER**

*Clutter* is the term used by radar engineers to denote *unwanted* echoes from the natural environment. It implies that these unwanted echoes "clutter" the radar and make difficult the detection of wanted targets. Clutter includes echoes from land, sea, weather (particularly rain), birds, and insects. At the lower radar frequencies, echoes from ionized meteortrails and aurora also can produce clutter. The electronic warfare technique known as *chaff* although not an example of the natural environment is usually considered as clutter since it is unwanted and resembles clutter from rain. Clutter is generally distributed in spatial extent in that it is much larger in physical size than the radar resolution cell. There is also "point," or discrete, clutter echoes, such as TV and water towers, buildings, and other similar structures that produce large backscatter. Large clutter echoes can mask echoes from desired targets and limit radar capability. When clutter is much larger than receiver noise, the optimum radar waveform and signal processing can be quite different from that employed when only receiver noise is the dominant limitation on sensitivity.

### **2.1.2 Target echoes**

The target induces a Doppler shift in the return signal. The magnitude of Doppler shift is proportional to the velocity of the target.

### **2.1.3 Noise**

Noises from various origins and of various pdf's are added to the radar signal in the space and radar receiver. They can effect different bands of frequency spectrum, also when white noise passes through IF amplifiers its distribution is changed to Raleigh.

## 2.1.4 EM interference

Interference signals from enemy as well as friendly sources are received by radar unless the interfering frequency is known by the radar. It can also cause malfunctioning of the radar.

## 2.2 RADAR BLOCK DIAGRAM

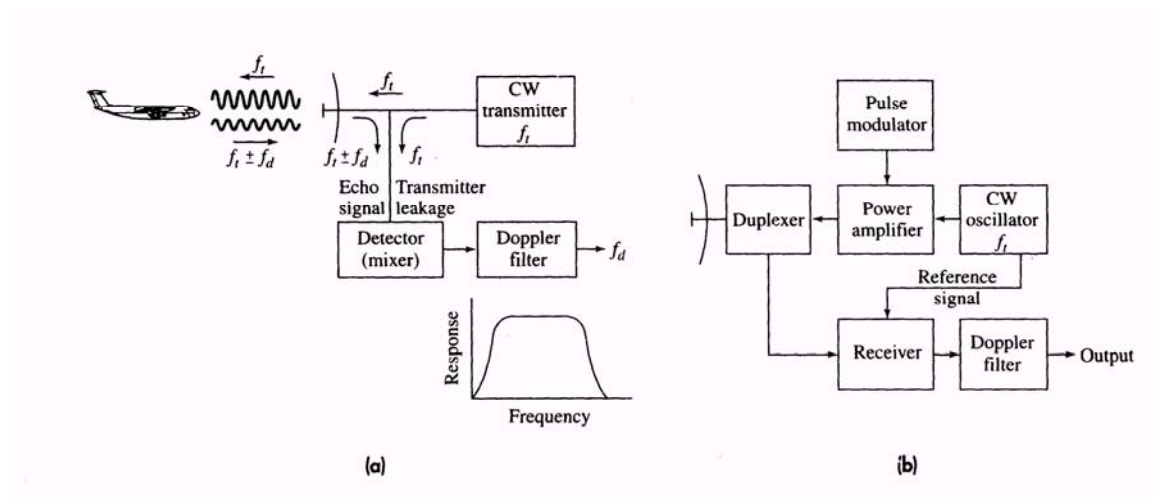


Figure 2.1(a) Simple CW radar block diagram that extracts the Doppler frequency shift from a moving target and rejects stationary clutter echoes. The frequency response of the Doppler filter is shown at the lower right, (b) Block diagram of simple pulse radar that extracts the Doppler frequency shift of the echo signal from a moving target. [3]

## 2.3 RADAR CROSS SECTION OF TARGETS

The radar cross-section  $\sigma$  is the property of a scattering object, or target, that is included in the radar equation to represent the magnitude of the echo signal returned to the radar by the target. The radar cross section is defined as

$$\text{Reradiated power density back at the radar} = \frac{P_t G}{4\pi R^2} \cdot \frac{\sigma}{4\pi R^2} \quad [2.2]$$

A definition of the radar cross section found in some texts on electromagnetic scattering is

$$\sigma = \frac{\text{power reflected toward source/unit solid angle}}{\text{incident power density}/4\pi} = 4\pi R^2 \frac{|E_r|^2}{|E_i|^2} \quad [2.3]$$

Where  $R$  is the range to the target,  $E_r$  is the electric field strength of the echo signal back at the radar, and  $E_i$  is the electric field strength incident on the target. It is assumed in the above that the target is far enough from the radar that the incident wave can be considered to be planar rather than spherical. Equation (2.1) is equivalent to the simple form of the radar equation. Sometimes the radar cross section  $\sigma$  is said to be a (fictional) area that intercepts a part of the power incident at the target which, if scattered uniformly in all directions, produces an echo power at the radar equal to that produced at the radar by the real target. Real targets, of course, do not scatter the incident energy uniformly in all directions.

The power scattered from a target in the direction of the radar receiver, and hence the radar cross section, can be calculated by solving Maxwell's equations with the proper boundary conditions applied or by computer modeling. The radar cross section can also be measured, based on the radar equation, using either full-size or scale models of targets. Radar cross section depends on the characteristic dimensions of the object compared to the radar wavelength. When the wavelength is large compared to the object's dimensions, scattering is said to be in the *Rayleigh region*. It is named after Lord Rayleigh who first

observed this type of scattering in 1871, long before the existence of radar, when investigating the scattering of light by microscopic particles. The radar cross section in the Rayleigh region is proportional to the fourth power of the frequency, and is determined more by the volume of the scatterer than by its shape. At radar frequencies, the echo from rain is usually described by Rayleigh scattering.

At the other extreme, where the wavelength is small compared to the object's dimensions, is the *optical region*. Here radar scattering from a complex object such as an aircraft is characterized by significant changes in the cross section when there is a change in frequency or aspect angle at which the object is viewed. Scattering from aircraft or ships at microwave frequencies generally is in the optical region. In the optical region, the radar cross section is affected more by the shape of the object than by its projected area.

In between the Rayleigh and the optical regions is the *resonance region* where the radar wavelength is comparable to the object's dimensions. For many objects, the radar cross section is larger in the resonance region than in the other two regions. These three distinct scattering regions are illustrated by scattering from the sphere.[2]

## 2.4 SYSTEM LOSSES

One of the important factors omitted from the simple radar equation was the loss that occurs throughout the radar system. The loss due to the integration of pulses and the loss due to a target with a fluctuating cross section have been already encountered. This section considers the various *system losses*, denoted  $L_s$  not included elsewhere in the radar equation. Some system losses can be predicted beforehand (such as losses in the transmission line); but others cannot (such as degradation when operating in the field). The latter must be estimated based on experience and experimental observations. They are subject to considerable variation and uncertainty. Although the loss associated with any one factor may be small, there can be many small effects that add up and result in significant total loss. The radar designer, of course, should reduce known losses as much as possible in the design and development of the radar. Even with diligent efforts to reduce losses, it is not unusual for the system loss to vary from perhaps 10 dB to more than 20 dB. (A 12-dB loss reduces the range by one-half.)

All numerical values of loss mentioned in this section, including the above values of system loss, are meant to be illustrative. They can vary considerably depending on the radar design and how the radar is maintained.

System loss,  $L_s$  (a number greater than one), is inserted in the denominator of the radar equation. It is the reciprocal of efficiency (number less than one). The two terms (loss and efficiency) are sometimes used interchangeably.

## 2.5 FINAL RADAR EQUATION

The simple form of the radar equation is,

$$R_{\max}^4 = \frac{P_{\text{av}} G A \rho_a \sigma n E_i(n) F^4 e^{-2\alpha R_{\max}}}{(4\pi)^2 k T_0 F_n (B\tau) f_p (S/N)_1 L_f L_s}$$

[2.4]

Where

$R_{\max}$  = Maximum radar range,  $m$

$P_{\text{av}}$  = Average transmitter power,  $W$

$G$  = Antenna gain

$A$  = Antenna area,  $m^2$

$\rho_a$  = Antenna aperture efficiency

$\sigma$  = Radar cross section of the target,  $m^2$

$n$  = Number of pulses integrated

$E_i(n)$  = Integration efficiency

$F^4$  = Propagation factor

$\alpha$  = Attenuation coefficient, nepers per unit distance

$k$  = Boltzmann's constant =  $1.38 \times 10^{-23}$  J/deg

$T_0$  = Standard temperature = 290 K

$F_n$  = Receiver noise figure

**$B$  = Receiver bandwidth, Hz**

**$\tau$  = Pulse width, s**

**$fp$  = Pulse repetition frequency, Hz**

**$(S/N)_I$  = Signal-to-noise ratio required as if detection were based on only a single pulse**

**$L_f$  = Fluctuation K loss (for a Swerling target model)**

**$L_s$  = System loss**

# Chapter 2

## PULSE DOPPLER RADAR

### 3.1 Doppler Frequency Shift

The doppler effect used in radar is the changing pitch of an audible siren from emergency vehicle as it travels toward or away from the listener. Here we are interested in the doppler effect that changes the frequency of the electromagnetic signal that propagates from the radar to a moving target and back to the radar. If the range to the target is  $R$ , then the total number of wavelengths  $\lambda$  in the two-way path from radar to target and return is  $2R/\lambda$ . Each wavelength corresponds to a phase change of  $2\pi$  radians. The total phase change in the two-way propagation path is then

$$\Phi = 2\pi \times \frac{2R}{\lambda} = 4\pi \frac{R}{\lambda} \quad [3.1]$$

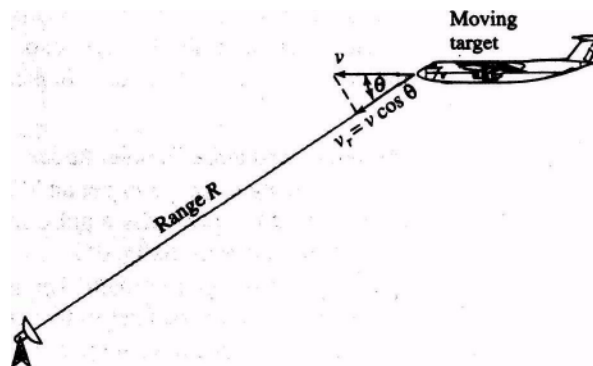


Figure 3.1(Geometry of radar and target in deriving the Doppler frequency shift.

Radar, target, and direction of target travel all lie in the same plane in this illustration.) [1]

If the target is in motion relative to the radar,  $R$  is changing and so will the phase. Differentiating Eq. (3.1) with respect to time gives the rate of change of phase, which is angular frequency

$$\omega_d = \frac{d\phi}{dt} = \frac{4\pi}{\lambda} \frac{dR}{dt} = \frac{4\pi v_r}{\lambda} = 2\pi f_d \quad [3.2]$$

where  $v_r = dR/dt$  is the radial velocity (meters/second), or rate of change of range with time. If, as in Fig. 3.1, the angle between the target's velocity vector and the radar line of sight to the target is  $\theta$ , then  $v_r = v \cos \theta$ , where  $v$  is the speed, or magnitude of the vector velocity. The rate of change of  $\Phi$  with time is the angular frequency  $\omega_d = 2\pi f_d$  where  $f_d$  is the *doppler frequency shift*. Thus from Eq. (3.2),

$$f_d = \frac{2 v_r}{\lambda} = \frac{2 f_t v_r}{c} \quad [3.3]$$

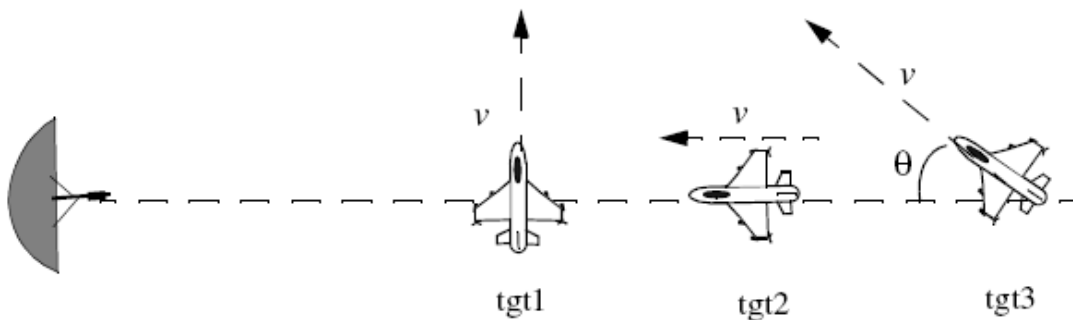


**Figure 3.2 Target 1 generates zero Doppler. Target 2 generates maximum Doppler. Target 3 is in-between. [1]**



The radar frequency is  $f_r = c/\lambda$ , and the velocity of propagation  $c = 3 \times 10^8$  m/s. If the doppler frequency is in hertz, the radial velocity in knots (abbreviated kt), and the radar wavelength in meters, we can write

$$f_d(\text{Hz}) = \frac{1.03v_r(\text{kt})}{\lambda(\text{m})} = \frac{v_r(\text{kt})}{\lambda(\text{m})} \quad [3.4]$$

### 3.2 Pulse Repetition Frequency

The pulse repetition frequency (prf) is often determined by the maximum unambiguous range beyond which targets are not expected. The prf corresponding to a maximum unambiguous range,  $R_{un}$  is given by  $prf = 2 R_{un}/c$ , where  $c$  is the velocity of propagation. There are times, however, when echoes might appear from beyond the maximum unambiguous range, especially for some unusually large target or clutter source (such as a mountain), or when anomalous propagation conditions occur to extend the normal range of the radar beyond the horizon. Echo signals that arrive at a time later than the pulse-repetition period are called *second-time-around echoes*. They are also called *multiple-time-around echoes*, particularly when they arrive from ranges greater than  $2R_{un}$ . The apparent range of these ambiguous echoes can result in error and confusion.

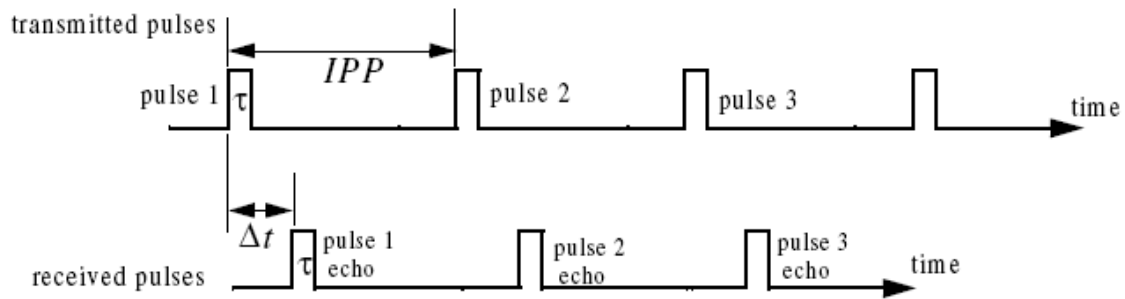


Figure 3.3. Train of transmitted and received pulses. [3]

Another problem with multiple-time-around echoes is that clutter echoes from ranges greater than  $R_{un}$  can mask unambiguous target echoes at the shorter ranges.

### 3.3 Range Bin

Pulse Repetition Interval (PRI) is divided by pulse width which granulizes the interval. Each of the of the differential segment is referred as range bin

### 3.4 Grazing Angle

The angle at which the radar antennas beam strikes the earth surface is called grazing angle.

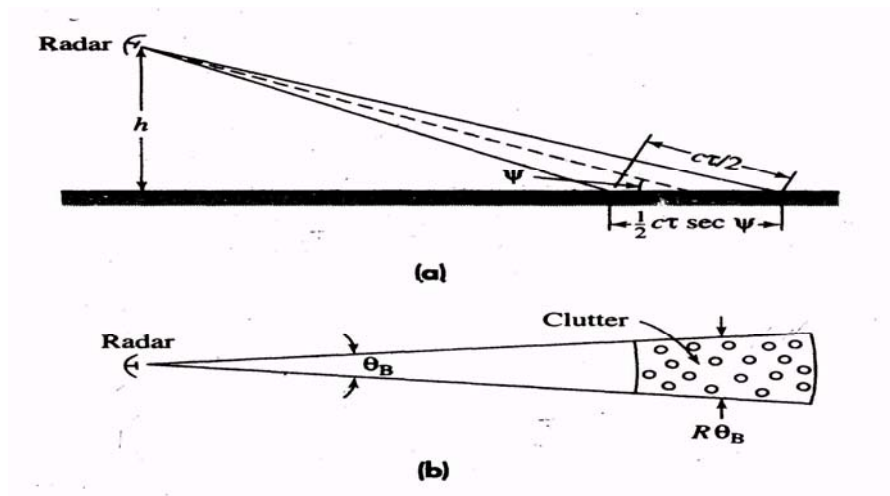


Figure 3.4 .Radar Geometry of radar surface clutter, (a) Elevation view showing the extent of the surface illuminated by the radar pulse, (b) plan view showing the illuminated clutter patch (or resolution cell) consisting of individual, independent scatterers.

### 3.5 Signal (Rx and Tx)

Pulse Radar That Extracts the Doppler Frequency-Shifted Echo Signal One cannot simply convert the CW radar of Fig. 2.1 to pulse radar by turning the CW oscillator on and off to generate *pulses*. *Generating pulses in this manner also removes* the reference signal at the receiver, which is needed to recognize that a Doppler frequency shift has occurred. The output of a stable CW oscillator is amplified by a high-power amplifier. The amplifier is turned on and off (modulated) to generate a series of high-power pulses. The received echo signal is mixed with the output of the CW oscillator which acts as a ***coherent reference*** to allow recognition of any change in the received echo-signal frequency. By ***coherent*** is meant that the phase of the transmitted pulse is preserved in the reference signal. The change in frequency is detected (recognized) by the Doppler filter.

If the transmitted signal of frequency  $f_t$  is represented as  $A_t \sin(2\pi f_t t)$ , the received signal is  $A_r \sin[2\pi f_t (t - T_R)]$ , where  $A_t$  = amplitude of transmitted signal and  $A_r$  = amplitude of the received echo signal. The round-trip time  $T_R$  is equal to  $2R/c$ , where  $R$  = range and  $c$  = velocity of propagation. If the target is moving toward the radar, the range is changing and is represented as  $R = R_o - v_r t$ , where  $v_r$  = radial velocity (assumed constant). The geometry is the same as was shown in Fig. 3.1. With the above substitutions, the received signal is

$$V_{\text{rec}} = A_r \sin \left[ 2\pi f_t \left( 1 + \frac{2v_r}{c} \right) t - \frac{4\pi f_t R_o}{c} \right] \quad [3.5]$$

The received frequency changes by the factor  $2f_t v_r/c = 2v_r/\lambda$  which is the Doppler frequency shift  $f_d$ . If the target had been moving away from the radar, the sign of the doppler frequency would be minus, and the received frequency would be less than that transmitted.

The received signal is heterodyned (mixed) with the reference signal  $A_{\text{ref}} \sin 2\pi f_t t$  and the difference frequency is extracted, which is given as

$$V_d = A_d \cos (2\pi f_d t - 4\pi R_o/\lambda) \quad [3.6]$$

where  $A_d$  = amplitude,  $f_d = 2 v_r/\lambda$  = Doppler frequency, and the relation  $f \lambda = c$  was used. (The cosine replaces the sine in the trigonometry of the heterodyning process.) For stationary targets  $f_d = 0$  and the output signal is constant. Since the sine takes on values from +1 to -1, the sign of the clutter echo amplitude can be minus as well as plus. On the other hand, the echo signal from a moving target results in a time-varying output (due the Doppler shift), which is the basis for rejecting stationary clutter echoes (with zero doppler frequency) but allowing moving-target echoes to pass. If the radar pulse width is long enough and if the target's doppler frequency is large enough, it may be possible to detect the Doppler frequency shift on the basis of the frequency change within a single pulse. If Fig. 3.5a represents *the* RF (or IF) echo pulse train. Fig. 3.5b is the pulse train when there is a recognizable Doppler frequency shift. To detect a Doppler shift on the basis of a single pulse of width  $\tau$  generally requires that there be at least one cycle of the Doppler frequency  $f_d$  within the pulse; or that  $f_d\tau > 1$ . This condition, however, is not usually met when detecting aircraft since the Doppler frequency  $f_d$  is generally much smaller than  $1/\tau$ . Thus the doppler effect cannot be utilized with a *single* short pulse in this case. Figure 3.5c is more representative of the doppler frequency for aircraft-detection radars. The doppler is shown sampled at the pulse repetition frequency (prf). More than one pulse is needed to recognize a change in the echo frequency due to the doppler effect. (Figure 3.5c is exaggerated in that the pulse width is usually small compared to the pulse repetition period. For example,  $\tau$  might be of the order of  $1\mu s$ , and the pulse repetition period might be of the order of  $1 ms$ .)

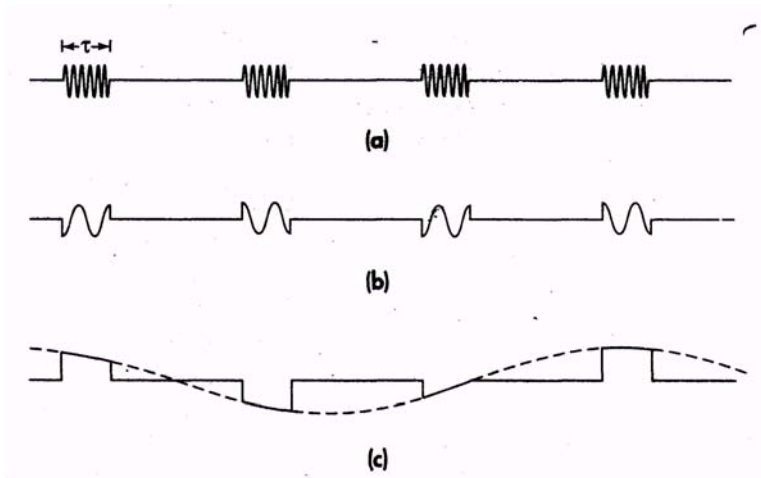


**Figure 3.5 (a) Representation of the echo pulse train at either the RF or IF portion of the receiver; (b) video pulse train after the phase detector when the doppler frequency [3]**

# Chapter 4

## SIGNAL PROCESSING

### 4.1 Detection

Radar *detects the presence* of an echo signal reflected from a target and *extracts information* about the target (such as its location). Methods for the detection of desired signals and the rejection of undesired noise, clutter, and interference in radar are called *signal processing*. The matched filter, is an important example of a radar signal processor.

### 4.2 Matched-Filter Receiver

Under certain conditions, usually met in practice, maximizing the output peak-signal-to-noise (power) ratio of a radar receiver maximizes the detect ability of a target. A linear network that does this is called a *matched filter*. Thus a matched filter, or a close approximation to it, is the basis for the design of almost all radar receivers.

**Matched Filter Impulse Response** The matched filter may also be described by its *impulse response*  $h(t)$ , which is the inverse Fourier transform of the frequency response function  $H(f)$  of Eq below ,

$$h(t) = \int_{-\infty}^{\infty} H(f) \exp(j2\pi ft) df = G_a \int_{-\infty}^{\infty} S^*(f) \exp[-j2\pi f(t_m - t)] df \quad [4.1]$$

Since  $S^*(f) = S(-f)$ , So above Eq(3.7) becomes

$$h(t) = G_a \int_{-\infty}^{\infty} S(f) \exp[j2\pi f(t_m - t)] df = G_a s(t_m - t) \quad [4.2]$$

The expression on the far right comes from recognizing that the integral is an inverse Fourier transform. Equation above indicates that the impulse response of a matched filter is the time inverse of the received signal. It is the received signal reversed in time  $t_m$  starting from the fixed time (Figure below shows an example of the impulse response  $h(t)$  of the Filter matched to a signal  $s(t)$ ).

The impulse response of a filter, if it is to be realizable, must not have any output before the input signal is applied. Therefore, we must have  $(t_m - t) > 0$ , or  $t < t_m$ . This is equivalent to the condition on the frequency response function that there be a phase  $\exp(-j2\pi f t_m)$ , which implies a time delay of  $t_m$ . For convenience, the impulse response is often written simply as  $s(-t)$  and the frequency response function as  $S^*(f)$ , with the realizability conditions understood.

### 4.3 Receiver Bandwidth

The matched filter is implemented in the IF stage of a superheterodyne receiver since the bandwidth of a superheterodyne receiver is essentially that of the IF- (The bandwidths of the RF and the mixer stages are usually large compared to that of the IF.) Thus the maximum signal-to-noise ratio occurs at the output of the IF. The second detector and the video portion of the receiver have negligible effect on the output signal-to-noise ratio if the video bandwidth is greater than one half the IF bandwidth.

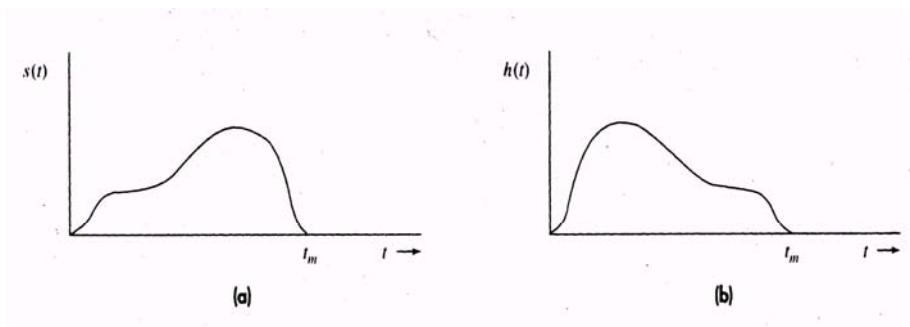


**Figure 4.1 (a) Example of received waveform  $s(t)$  (b) impulse response  $h(t)$  of the matched filter for the input signal. [4]**

## 4.4 Detection Criteria

Detection of signals is equivalent to deciding whether the receiver output is due to noise alone or to signal plus noise. This is the type of decision made (probably subconsciously) by a human operator from the information presented on a radar display. When the detection process is carried out automatically by electronic means without the aid of an operator, the detection criterion must be carefully specified and built into the decision-making device.

If the envelope of the receiver output exceeds a pre-established threshold, a signal is said to be present. The threshold level divides the output into a region of no detection and a region of detection. The radar engineer selects the threshold that divides these two regions so as to achieve a specified probability of false alarm, which in turn is related to the average time between false alarms. The engineer then determines the other parameters of the radar needed to obtain the signal-to-noise ratio for the desired probability of detection. [5]

### 4.4.1 Neyman-Pearson

The usual procedure for establishing the decision threshold at the output of the radar receiver is based on the classical statistical theory of the *Neyman-Pearson observer*. This is described in terms of the two types of errors that might be made in the detection decision process.

One type of error is to mistake noise for signal when only noise is present. It occurs whenever the noise out of the receiver is large enough to exceed the decision-threshold level. In statistics this is called a Type I error. In radar it is a *false alarm*. A Type II error occurs when a signal is present, but is erroneously considered to be noise. The radar engineer would call such an error a *missed detection*.

### 4.4.2 Likelihood-Ratio Receiver

The *likelihood ratio* is a statistical concept that has been used in radar detection theory and information extraction theory to model optimum decision procedures. It is defined as the ratio of two probability density functions, with and without signal present, or

$$L_r(\mathbf{v}) = p_{sn} / p_n$$



where  $p_{sn}$  is the probability-density function for signal plus noise and  $p_n$  is the probability density function for noise alone.

## 4.5 Detectors

The detector is that portion of the radar receiver that extracts the modulation from the carrier in order to decide whether or not a signal is present. It extends from the IF amplifier to the output of the video amplifier; thus, it is much more than a rectifying element.

### 4.5.1 Optimum Envelope Detector Law

The envelope detector consists of the IF amplifier with band pass filter characteristic, a rectifying element (such as a diode), and a video amplifier with a low-pass filter characteristic. The detector is called a *linear detector* if the relation between the input and output signal is linear for positive voltage signals, and zero for negative voltage. (The detector, of course, is a nonlinear device even though it bears the name *linear*.) When the output is the square of the input for positive voltage, the detector is called *square law*.

### 4.5.2 Logarithmic Detector

If the output of the receiver is proportional to the logarithm of the input envelope, it is called a *logarithmic detector*, or *logarithmic receiver*. It finds application where large variations of input signals are expected.

### 4.5.3 I,Q Detector

The I and Q, or *in-phase* and *quadrature*, channels were mentioned in the discussion of the MTI radar. There it was noted that a single phase-detector fed by a coherent reference could produce a significant loss in signal depending on the relative timing (or "phase") of the pulse train and the Doppler-shifted echo signal. In MTI radar, the term *blind phase* (not a truly descriptive term) was used to describe this loss.

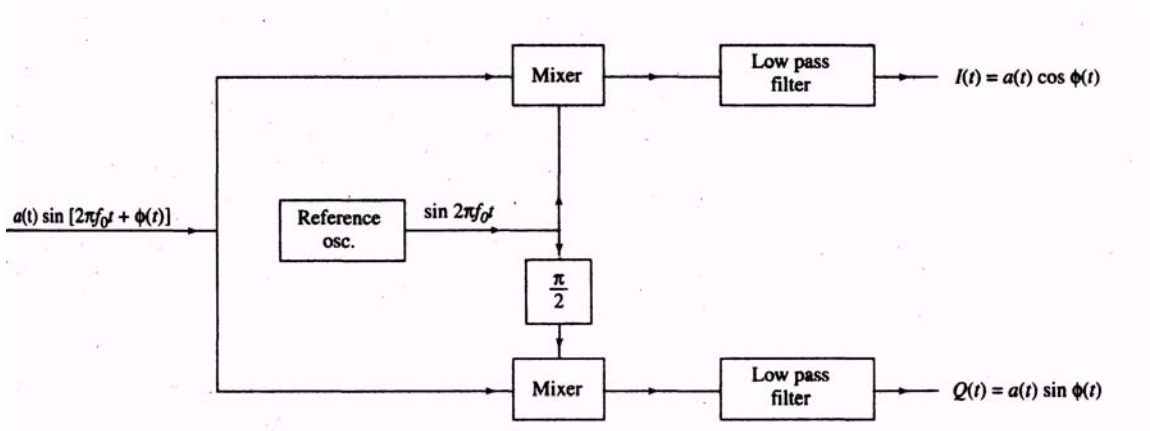


Figure 4.2 I ,Q Demodulation [3]

#### 4.5.4 Coherent Detector

The so-called "coherent detector" sometimes has been described in the past literature as a single-channel detector similar to the in-phase channel of the  $I,Q$  detector, but with the reference signal at the same exact frequency and same exact phase as that of the input signal. Compared to the normal envelope detector, the signal-to-noise ratio from a coherent detector might be from 1 to 3 dB greater. Unfortunately, the phase of the received radar signal is seldom known, so the single-channel coherent detector as described generally is not applicable to radar. The  $I, Q$  detector of Fig. above can also be considered as a coherent detector, but without the limitation of the coherent detector described above.

#### 4.6 Clutter Filtering

*Clutter* is the term used by radar engineers to denote *unwanted* echoes from the natural environment. It implies that these unwanted echoes "clutter" the radar and make difficult the detection of wanted targets. Clutter includes echoes from land, sea, weather (particularly rain), birds, and insects. At the lower radar frequencies, echoes from ionized meteor trails and aurora also can produce clutter. The electronic warfare technique known as *chaff*, although not an example of the natural environment, is usually considered as

clutter since it is unwanted and resembles clutter from rain. Clutter is generally distributed in spatial extent in that it is much larger in physical size than the radar resolution cell. There are also "point." or discrete, clutter echoes, such as TV and water towers, buildings, and other similar structures that produce large backscatter. Large clutter echoes can mask echoes from desired targets and limit radar capability- When clutter is much larger than receiver noise, the optimum radar waveform and signal processing can be quite different from that employed when only receiver noise is the dominant limitation on sensitivity.

Radar echoes from the environment are not always undesired. Reflections from storm clouds, for example, can be a nuisance to a radar that must detect aircraft; bill storm clouds containing rain are what the radar meteorologist wants to detect in order to measure rain fall rate over a large area. The backscatter echoes from land can interfere with many applications of radar, but they are die target of interest for ground-mapping radar, synthetic aperture radars, and radars that observe earth resources. Thus the same environmental echo might he the desired signal in one application und the undesired clutter echo in another. The observation of land, sea weather and other natural phenomena by radar and other sensors for the purpose of determining something about the environment is known as *remote sensing of the environment*, or simply *remote sensing*. All radars, strictly speaking, are remote sensors; but the term is usually applied only to those radars; whose major function is to observe the natural environment for the purpose of extracting information about the environment, A prime example of a radar used for remote sensing is the Doppler weather radar.[5]

#### **4.6.1 Statistical Models for Surface Clutters**

Because of the highly variable nature of clutter echoes it is often described by a probability density function (pdf) or a probability distribution. This section describes several statistical models that have been suggested for characterizing the fluctuations of the surface-clutter cross section per unit area, or  $\sigma$ . They can apply to both sea and land clutter. The term *distribution*, as in *Raleigh distributions*, is used here to indicate the statistical nature of the phenomenon and applies to either the pdf or the probability

distribution function. In this chapter, however, the pdf rather than the probability distribution is usually used to describe clutter statistics.

#### 4.6.1.1 Rayleigh Distribution

This popular model is based on the assumption that there are a large number of randomly located independent scatterers within the clutter surface area illuminated by the radar- (The assumption of a large number is usually satisfied with as few as ten scatterers.) It is further assumed that none of the individual scatterers is significantly larger than the others.

If the radar receiver uses a linear detector, the probability density function of the voltage envelope of the Rayleigh distributed clutter at the receiver output is  $m_2$

$$p(v) = \frac{2v}{m_2} \exp\left(-\frac{v^2}{m_2}\right) \quad v \geq 0$$

#### 4.6.1.2 Log-Normal Distribution

As mentioned, the Rayleigh clutter model usually applies when the radar resolution cell is large so that it contains many scatterers, with no one scatterer dominant. It has been used to characterize relatively uniform clutter. However, it is not a good representation of clutter when the resolution cell size and the grazing angle are small. Under these conditions, there is a higher probability of getting large values of clutter (higher "tails") than is given by the Rayleigh model. One of the first models suggested to describe non-Rayleigh clutter was the log-normal pdf since it has a long tail (when compared to the Rayleigh). In the log-normal pdf the clutter echo power expressed in dB is Gaussian. [2]

$$p(P) = \frac{1}{\sqrt{2\pi sP}} \exp\left[-\frac{1}{2s^2} \left(\ln \frac{P}{P_m}\right)^2\right] \quad P \geq 0$$

## 4.7 Single Delay Line Canceller

A single delay line canceller can be implemented as shown in Fig. 3.8. The canceller's impulse response is denoted as  $h(t)$ . The output  $y(t)$  is equal to the convolution between the impulse response  $h(t)$  and the input  $x(t)$ . The single delay canceller is often called a "two-pulse canceller" since it requires two distinct input pulses before an output can be read. The delay  $T$  is equal to the PRI of the radar ( $1/f_r$ ). The output signal  $y(t)$  is

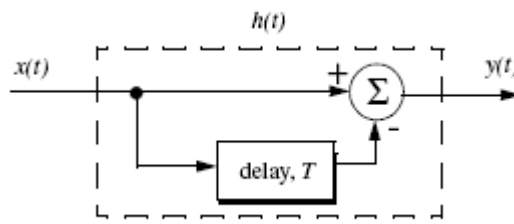


Fig4.3 Single delay line canceller.

$$y(t) = x(t) - x(t - T)$$

The impulse response of the canceler is given by

$$h(t) = \delta(t) - \delta(t - T)$$

where  $\delta(\cdot)$  is the delta function. It follows that the Fourier transform of  $h(t)$  is

$$H(\omega) = 1 - e^{-j\omega T}$$

where  $\omega = 2\pi f$ .

In the z-domain, the single delay line canceler response is

$$H(z) = 1 - z^{-1}$$

The power gain for the single delay line canceler is given by

$$|H(\omega)|^2 = H(\omega)H^*(\omega) = (1 - e^{-j\omega T})(1 - e^{j\omega T})$$

It follows that

$$|H(\omega)|^2 = 1 + 1 - (e^{j\omega T} + e^{-j\omega T}) = 2(1 - \cos\omega T)$$

and using the trigonometric identity  $(2 - 2\cos 2\vartheta) = 4(\sin \vartheta)^2$  yields

## 4.8 Double Delay Line Cancellor

Two basic configurations of a double delay line Cancellor are shown in Fig.3.9. Double Cancellers are often called “three-pulse Cancellers” since they require three distinct input pulses before an output can be read. The double line Cancellor impulse response is given by

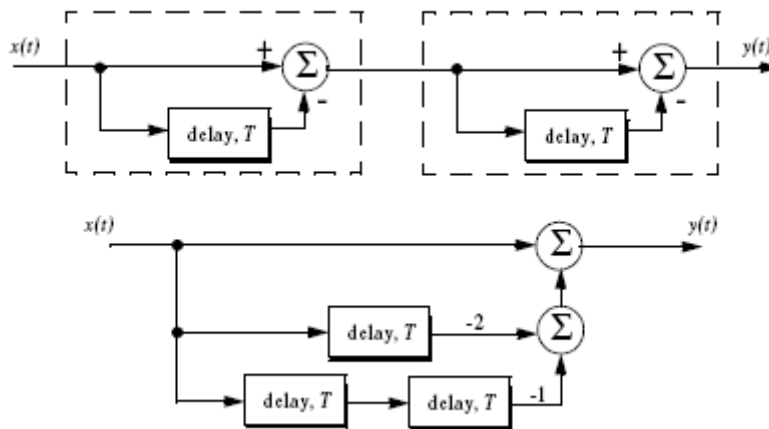
$$h(t) = \delta(t) - 2\delta(t - T) + \delta(t - 2T)$$

Again, the names “double delay line” Cancellor and “double canceller” will be used interchangeably. The power gain for the double delay line Cancellor is

$$|H(\omega)|^2 = |H_1(\omega)|^2 |H_1(\omega)|^2$$

Where  $|H(\omega)|^2$  is the single line Cancellor power gain. It follows that

$$|H(\omega)|^2 = 16 \left( \sin\left(\omega \frac{T}{2}\right) \right)^4$$



4.4 Two configurations for a double delay line Cancellor. [2]

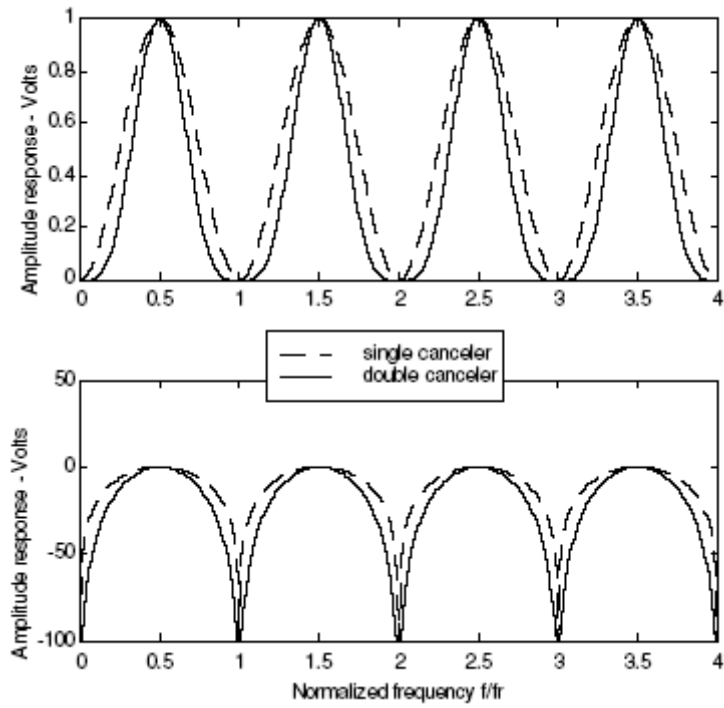


Figure 4.5 Normalized frequency responses for single and double cancellers. [2]

# Chapter 5

## Target Tracking

### 5.1 Single Target Tracking

Tracking radar systems are used to measure the target's relative position in range, azimuth angle, elevation angle, and velocity. Then, by using and keeping track of these measured parameters the radar can predict their future values. Target tracking is important to military radars as well as to most civilian radars. In military radars, tracking is responsible for fire control and missile guidance; in fact, missile guidance is almost impossible without proper target tracking. Commercial radar systems, such as civilian airport traffic control radars, may utilize tracking as a means of controlling incoming and departing airplanes. Tracking techniques can be divided into range/velocity tracking and angle tracking. It is also customary to distinguish between continuous single-target tracking radars and multi-target track-while-scan (TWS) radars. Tracking radars utilize pencil beam (very narrow) antenna patterns. It is for this reason that separate search radar is needed to facilitate target acquisition by the tracker. Still, the tracking radar has to search the volume where the target's presence is suspected. For this purpose, tracking radars use special search patterns, such as helical, T.V. raster, cluster, and spiral patterns, to name a few. Angle tracking is concerned with generating continuous measurements of the target's angular position in the azimuth and elevation coordinates. The accuracy of early generation angle tracking radars depended heavily on the size of the pencil beam employed. Most modern radar systems achieve very fine angular measurements by utilizing monopulse-tracking techniques.

Tracking radars use the angular deviation from the antenna main axis of the target within the beam to generate an error signal. This deviation is normally measured from the antenna's main axis. The resultant error signal describes how much the target has deviated from the beam main axis. Then, the beam position is continuously changed in an attempt to produce a zero error signal. If the radar beam is normal to the target



(maximum gain), then the target angular position would be the same as that of the beam. In practice, this is rarely the case. In order to be able to quickly achieve changing the beam position; the error signal needs to be a linear function of the deviation angle. It can be shown that this condition requires the beam's axis to be squinted by some angle (squint angle) off the antenna's main axis.

## **5.2 Multiple Target Tracking**

Track-while-scan radar systems sample each target once per scan interval, and use sophisticated smoothing and prediction filters to estimate the target parameters between scans. To this end, the Kalman filter and the Alpha-Beta-Gamma ( $\alpha\beta\gamma$ ) filter are commonly used. Once a particular target is detected, the radar may transmit up to a few pulses to verify the target parameters, before it establishes a track file for that target. Target position, velocity, and acceleration comprise the major components of the data maintained by a track file. The principles of recursive tracking and prediction filters are presented in this part. First, an overview of state representation for Linear Time Invariant (LTI) systems is discussed. Then, second and third order one-dimensional fixed gain polynomial filter trackers are developed. These filters are, respectively, known as the  $g-h$  and  $g-h-k$  filters (also known as the  $g-h$  and  $g-h-k$  filters).

Finally, the equations for an  $n$ -dimensional multi-state Kalman filter is introduced and analyzed. As a matter of notation, small case letters, with an underneath bar, are used.

### **5.2.1 Track-While-Scan (TWS)**

Modern radar systems are designed to perform multi-function operations, such as detection, tracking, and discrimination. With the aid of sophisticated computer systems, multi-function radars are capable of simultaneously tracking many targets. In this case, each target is sampled once (mainly range and angular position) during a dwell interval (scan). Then, by using smoothing and prediction techniques future samples can be estimated. Radar systems that can perform multi-tasking and multi-target tracking are known as Track-While-Scan (TWS) radars.

Once a TWS radar detects a new target it initiates a separate track file for that detection; this ensures that sequential detections from that target are processed together to estimate the target's future parameters. Position, velocity, and acceleration comprise the main components of the track file. Typically, at least one other confirmation detection (verify detection) is required before the track file is established.

Unlike single target tracking systems, TWS radars must decide whether each detection (observation) belongs to a new target or belongs to a target that has been detected in earlier scans. And in order to accomplish this task, TWS radar systems utilize correlation and association algorithms. In the correlation process each new detection is correlated with all previous detections in order to avoid establishing redundant tracks. If a certain detection correlates with more than one track, then a pre-determined set of association rules are exercised so that the detection is assigned to the proper track. A simplified TWS data processing block diagram is shown in Fig. 5.1.

Choosing a suitable tracking coordinate system is the first problem a TWS radar has to confront. It is desirable that a fixed reference of an inertial coordinate system be adopted. The radar measurements consist of target range, velocity, azimuth angle, and elevation angle. The TWS system places a gate around the target position and attempts to track the signal within this gate. The gate dimensions are normally azimuth, elevation, and range. Because of the uncertainty associated with the exact target position during the initial detections, a gate has to be large enough so that targets do not move appreciably from scan to scan; more precisely, targets must stay within the gate boundary during successive scans. After the target has been observed for several scans the size of the gate is reduced considerably.[5]

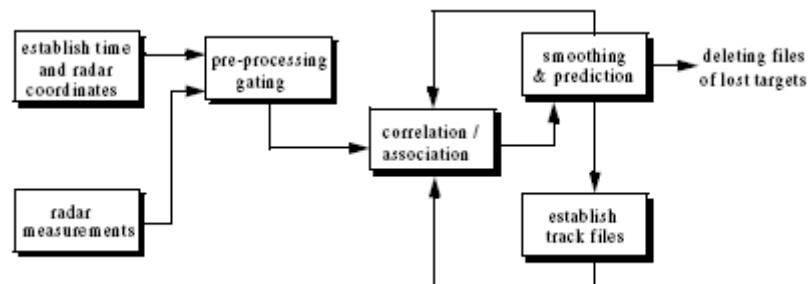


**Figure 5.1 Simplified block diagram of TWS data processing [5]**

Gating is used to decide whether an observation is assigned to an existing track file, or to a new track file (new detection). Gating algorithms are normally based on computing a statistical error distance between a measured and an estimated radar observation. For each track file, an upper bound for this error distance is normally set. If the computed difference for a certain radar observation is less than the maximum error distance of a given track file, then the observation is assigned to that track.

All observations that have an error distance less than the maximum distance of a given track are said to correlate with that track. For each observation that does not correlate with any existing tracks, a new track file is established accordingly. Since new detections (measurements) are compared to all existing track files, a track file may then correlate with no observations or with one or more observations. The correlation between observations and all existing track files is identified using a correlation matrix. Rows of the correlation matrix represent radar observations, while columns represent track files. In cases where several observations correlate with more than one track file, a set of predetermined association rules can be utilized so that a single observation is assigned to a single track file.

### 5.3 $\alpha\beta$ Filter

The  $\alpha\beta$  tracker produces, on the  $n$ th observation, smoothed estimates for position and velocity, and a predicted position for the  $(n+1)$ th observation. Fig. 5.1 shows an implementation of this filter. Note that the subscripts “ $p$ ” and “ $s$ ” are used to indicate, respectively, the predicted and smoothed values. The  $\alpha\beta$  tracker can follow an input ramp (constant velocity) with no steady state errors. However, a steady state error will accumulate when constant acceleration is present in the input. Smoothing is done to reduce errors in the predicted position through adding a weighted difference between the measured and predicted values to the predicted position, as follows:

$$x_s(n) = x(n|n) = x_p(n) + \alpha(x_0(n) - x_p(n))$$

$$\dot{x}_s(n) = x'(n|n) = \dot{x}_s(n-1) + \frac{\beta}{T} (x_0(n) - x_p(n))$$

$x_0$  is the position input samples. The predicted position is given by

$$x_p(n) = x_s(n|n-1) = x_s(n-1) + T\dot{x}_s(n-1)$$

The initialization process is defined by

$$x_s(1) = x_p(2) = x_0(1)$$

$$\dot{x}_s(1) = 0$$

$$\dot{x}_s(2) = \frac{x_0(2) - x_0(1)}{T}$$

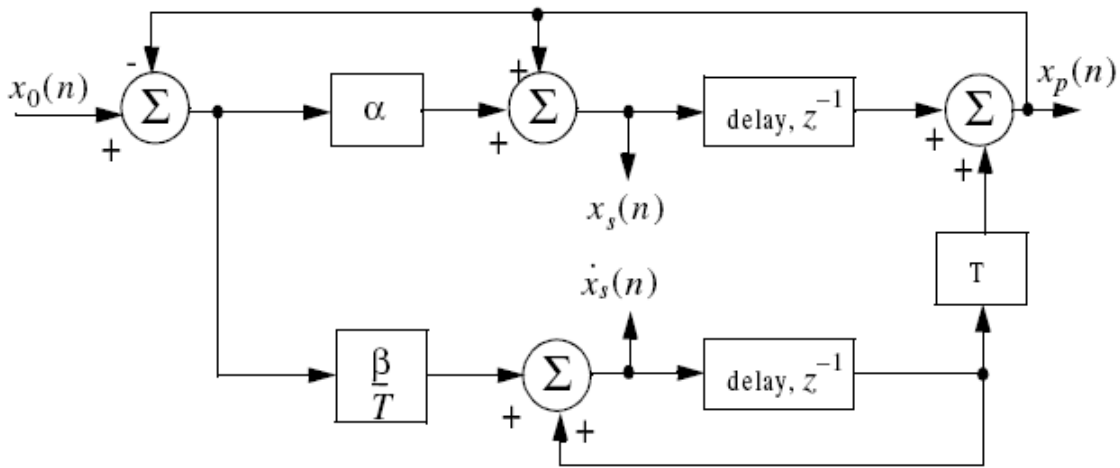


Figure 5.2 An implementation for an  $\alpha\beta$  tracker [5]

## 5.4 $\alpha\beta\gamma$ Filter

The  $\alpha\beta\gamma$  tracker produces, for the  $n$ th observation, smoothed estimates of position, velocity, and acceleration. It also produces predicted position and velocity for the  $(n+1)$ th observation. An implementation of the  $\alpha\beta\gamma$  tracker is shown in Fig. 5.2. The  $\alpha\beta\gamma$  tracker will follow an input whose acceleration is constant with no steady state errors. Again, in order to reduce the error at the output of the tracker, a weighted difference between the

measured and predicted values is used in estimating the smoothed position, velocity, and acceleration as follows:

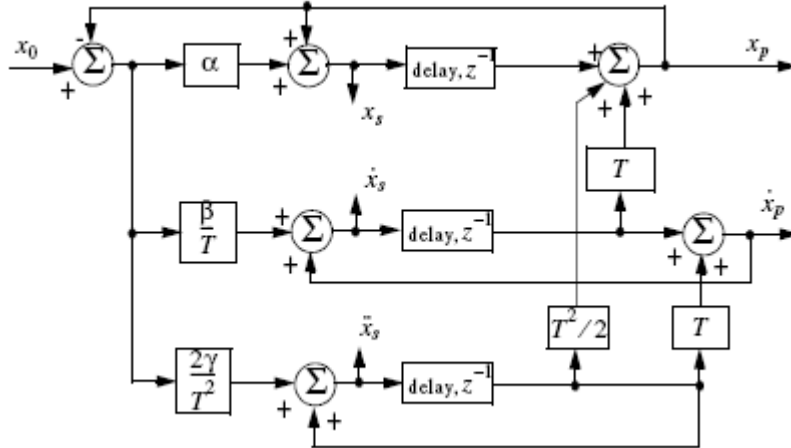


Figure 5.3 an implementation for an  $\alpha\beta\gamma$  tracker [5]

$$x_s(n) = x_p(n) + \alpha(x_0(n) - x_p(n))$$

$$\dot{x}_s(n) = \dot{x}_s(n-1) + T\ddot{x}_s(n-1) + \frac{\beta}{T} (x_0(n) - x_p(n))$$

$$\ddot{x}_s(n) = \ddot{x}_s(n-1) + \frac{2\gamma}{T^2} (x_0(n) - x_p(n))$$

$$x_p(n+1) = x_s(n) + T \dot{x}_s(n) + \frac{T^2}{2} \ddot{x}_s(n)$$

and the initialization process is

$$x_s(1) = x_p(2) = x_0(1)$$

$$\dot{x}_s(1) = \ddot{x}_s(1) = \ddot{x}_s(2) = 0$$

$$\dot{x}_s(2) = \frac{x_0(2) - x_0(1)}{T}$$

$$\ddot{x}_s(3) = \frac{x_0(3) + x_0(1) - 2x_0(2)}{T^2}$$

# Chapter 6

## SIMULATION

Our project dealt with the processing of a pulse Doppler radar signal with main aim of detection of targets and then establishing of track files associated with the target i.e. tracking. In the first part of project we simulated the whole process of detection in Matlab. The course of events run as follows

- Simulating the process of Doppler Recovery i.e. conversion of signal from IF stage to base band
- Simulating a comprehensive radar signal containing multiple targets, clutters, noise
- Processing of the generated data with the help of various algorithms

The second stage of work comprised of simulating the process of tracking of the detected targets .We preceded on the following lines

- Generation of the simulated radar data over multiple sweeps
- Detected the targets out of the generated file
- Established a track file for each of the detected target and updated it for every scan

Third and the final step was the processing of the original radar data for the detection purpose only.

Our project is primarily a comparative study of different algorithms that are used in detection and tracking of the target in a Pulse Doppler radar processor at the receiver.

That involved some of the current techniques in use.

## 6.1 Stage 1

### Doppler shift recovery (IF to Base Band Conversion)

We simulated a radar signal which has just entered the IF stage of the radar. It contained a single target or clutter depending on the Doppler shift induced together with the noise background. Then the signal was I, Q demodulated and down converted to the base band. The purpose of the simulation was to develop an idea that how the radar signal might look at the IF and base band stage of the radar.

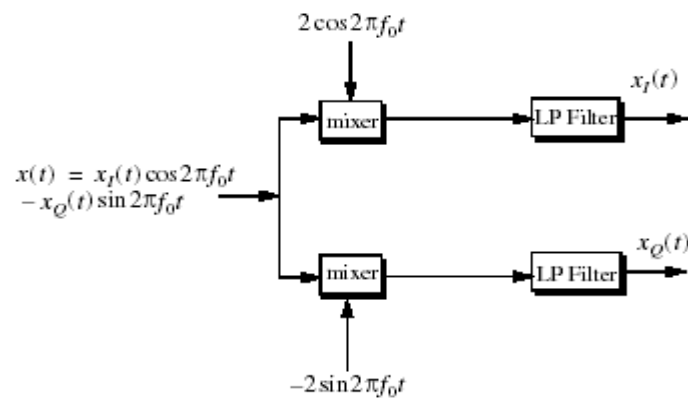


Fig 6.1 I/Q DEMODULATOR [5]

First the signal at IF stage of radar transmitter is shown. It contained the base band pulse train signal modulated by high frequency carrier signal.

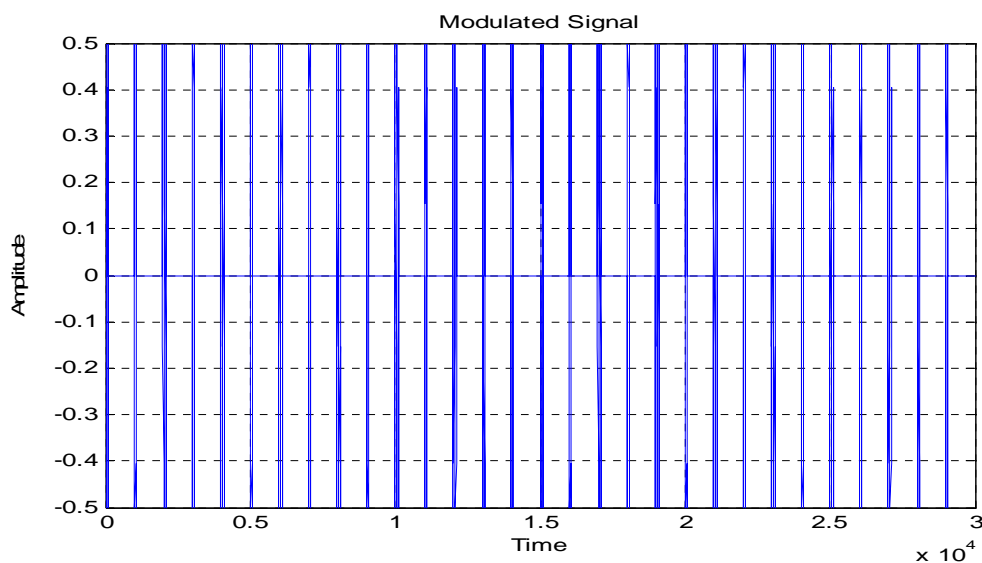
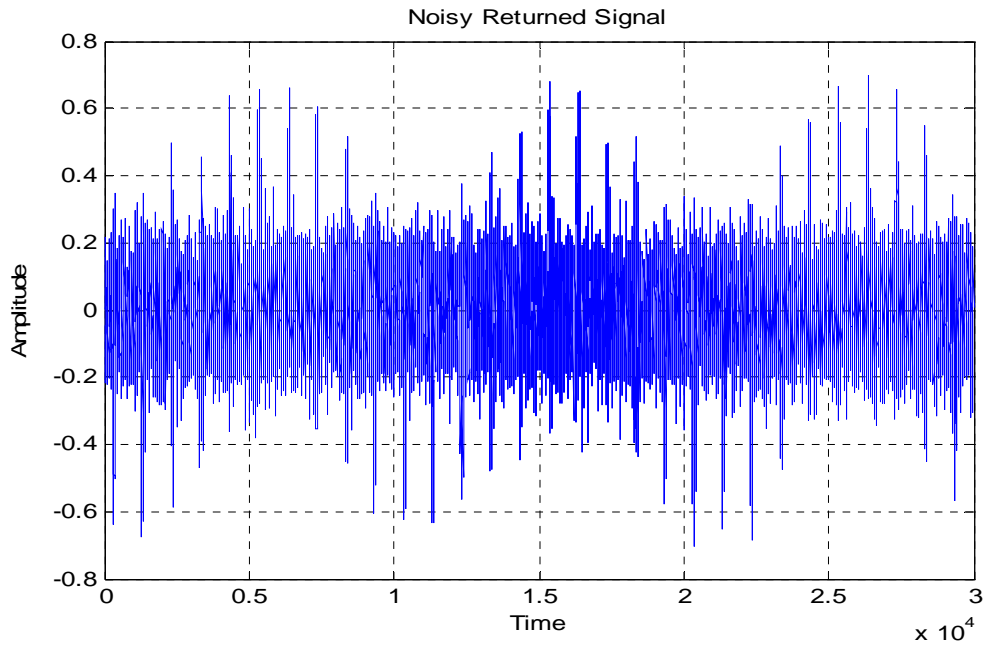


Fig 6.2 Transmitted Signal at IF stage [x]

It is up converted to the RF stage and transmitted. When it is reflected back, it is time shifted version of the transmitted signal but containing the Doppler shift and noise. It is then down-convert to IF stage.

The IF Stage signal having Doppler shift looks like



**Fig 6.3 Target Return [x]**

The return of the clutter will have no Doppler shift and look like this

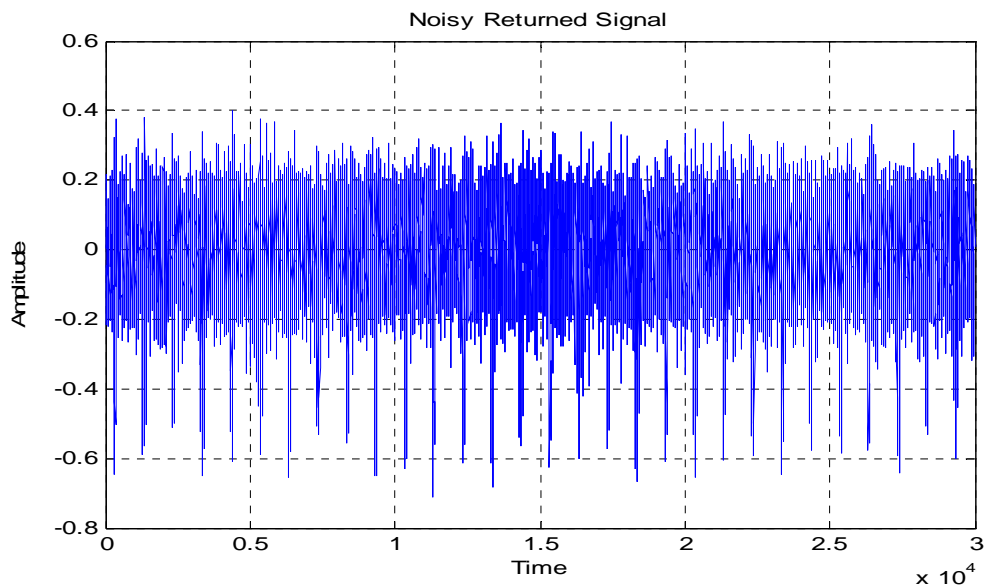


**Fig 6.4 Clutter Return [x]**



In the next step the IF signal is multiplied with In-Phase and In-quadrature carrier signal and low pass filtered to get base band signal. We used a windowed sinc Low Pas filter with a Blackman window to remove the carrier component. Then impulse and frequency response of filter

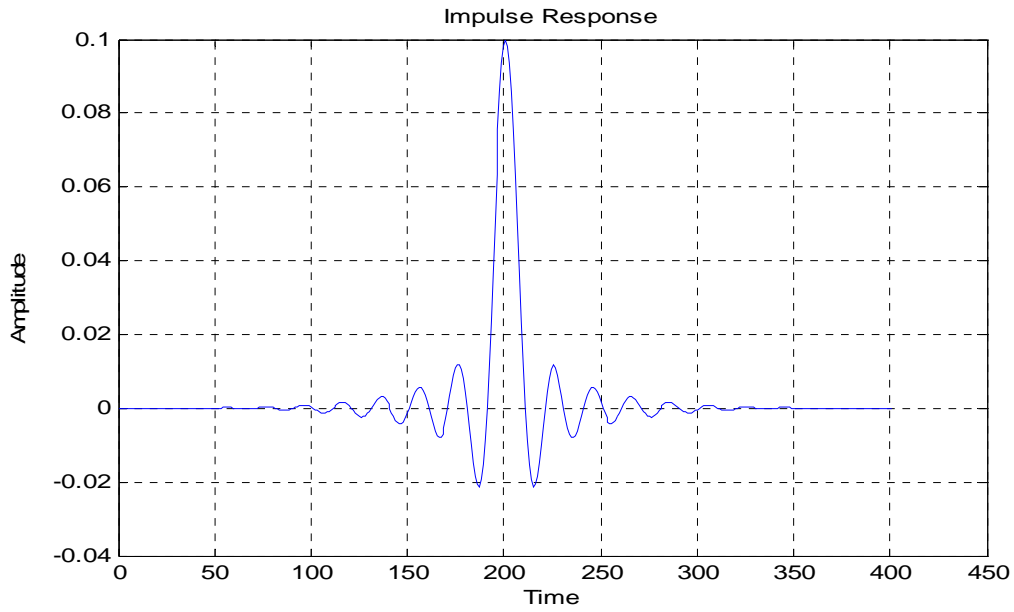


**Fig 6.5 Impulse Response of LPF [x]**

Frequency response of our low pass filter is given by

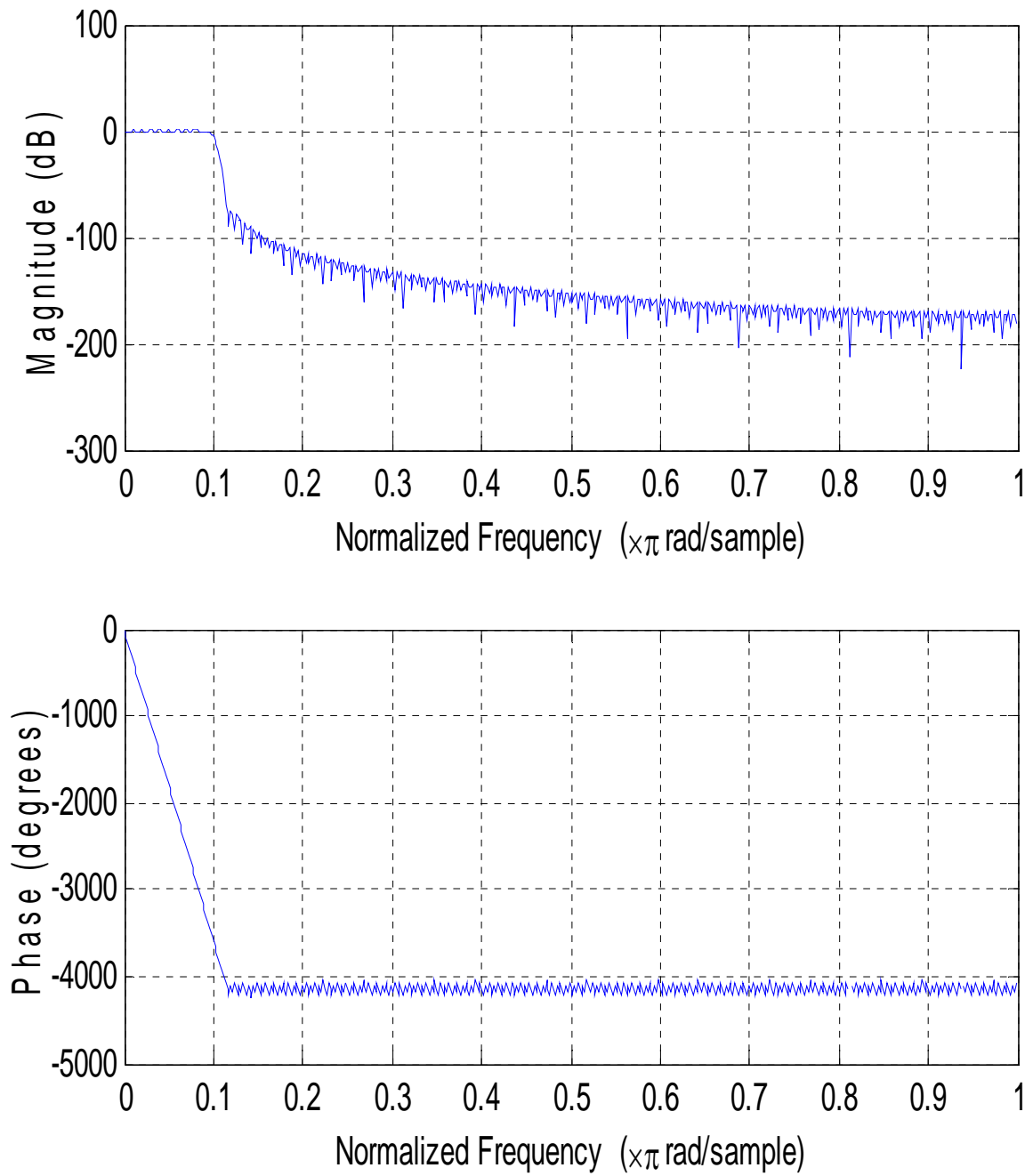


**Fig 6.6 Frequency Response of LPF [x]**

The outputs of the filter after down sampling the I and Q channels are

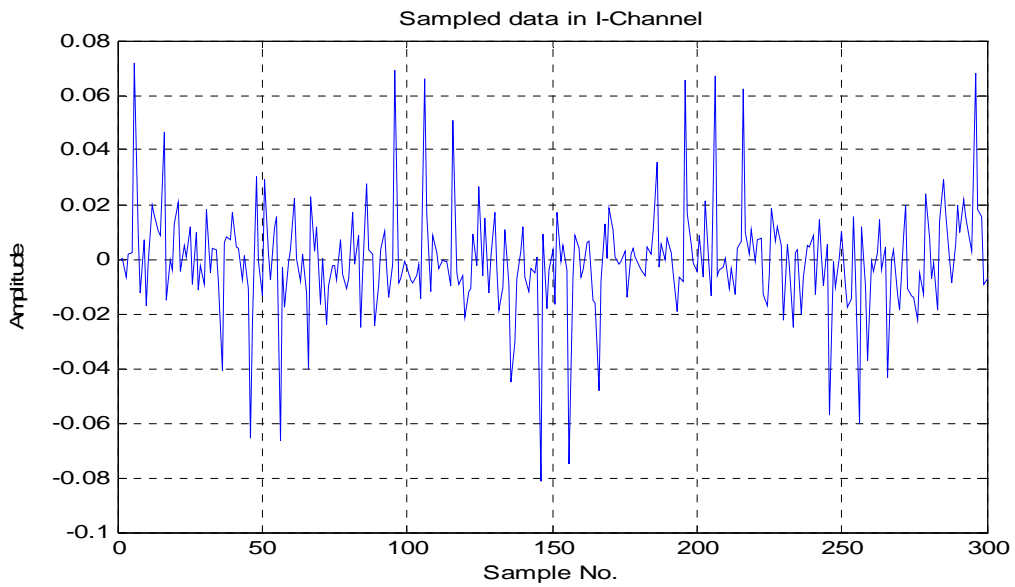


**Fig 6.7 Filtered & down sampled I channel Output for target [x]**

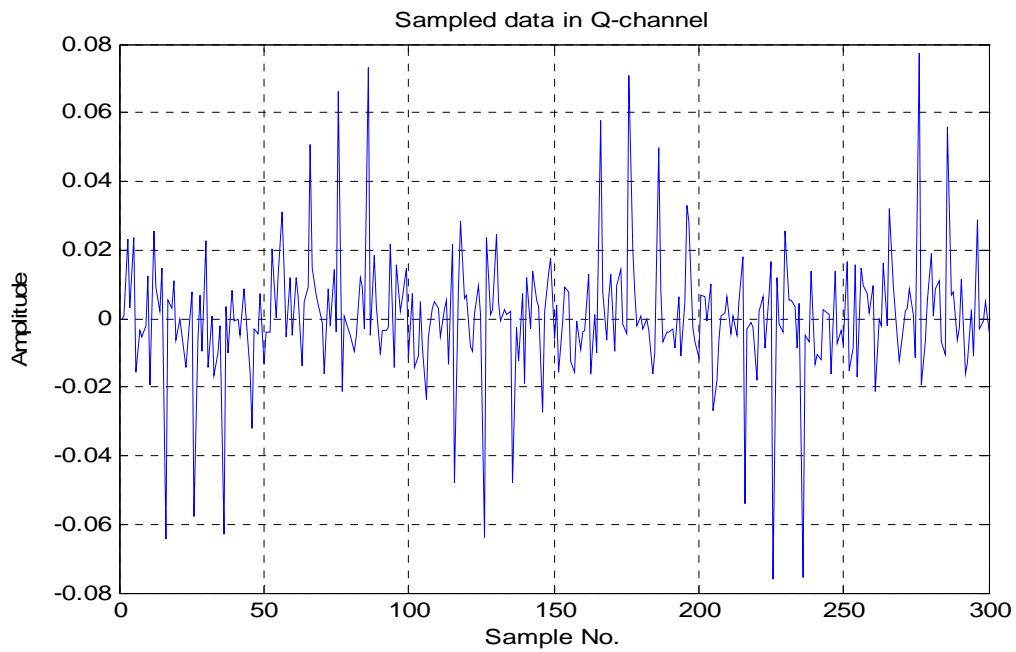


**Fig 6.8 Filtered & down sampled Q channel Output for target [x]**

For clutter the filtered and sampled output is given by

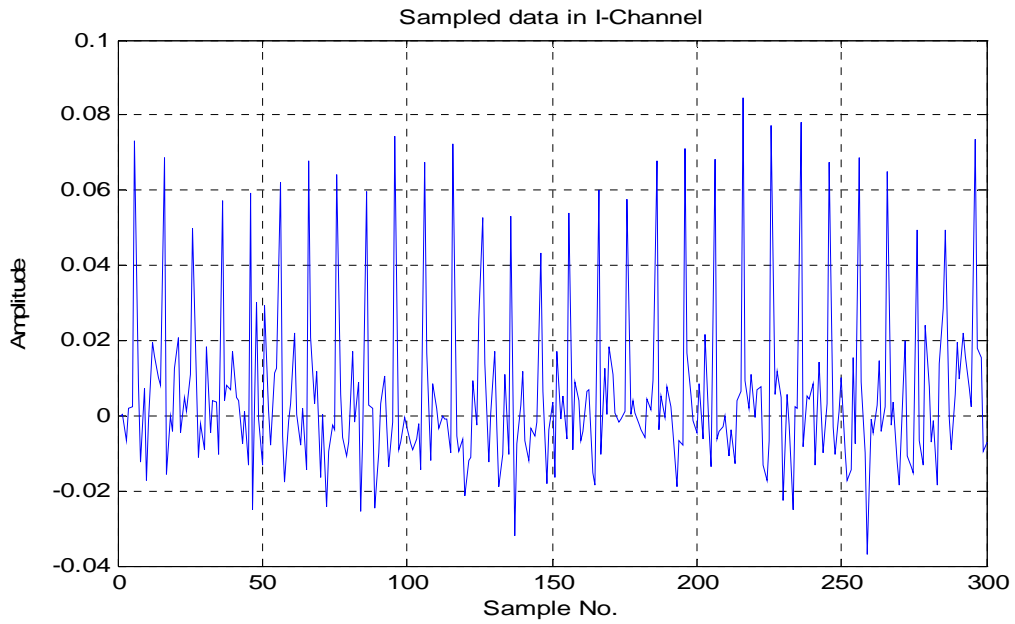


**Fig 6.9 Filtered & Down sampled I channel Output for clutter [x]**

For Q channel the output has only noise

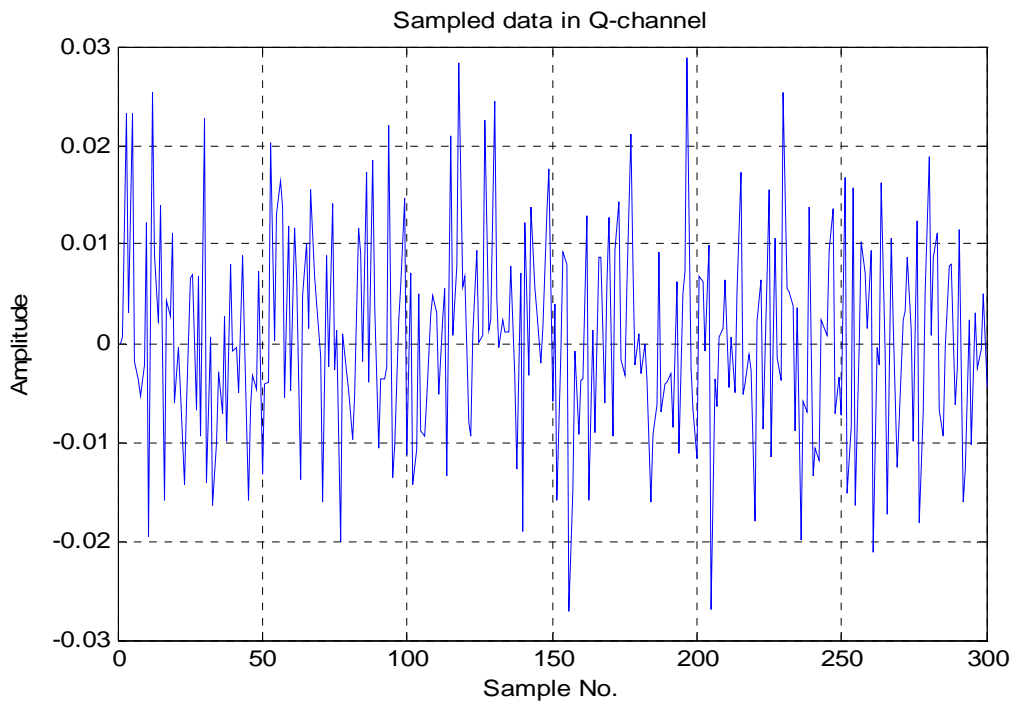


**Fig 6.10 Filtered & Down sampled Q channel Output for clutter [x]**

## 6.2 Stage 2

### Generation of a comprehensive radar base band signal

In the next stage we simulated a comprehensive radar signal containing multiple targets, clutters with different distributions and noise with different values of SNR and distributions. We provided the options to decorrelate the clutter in time.

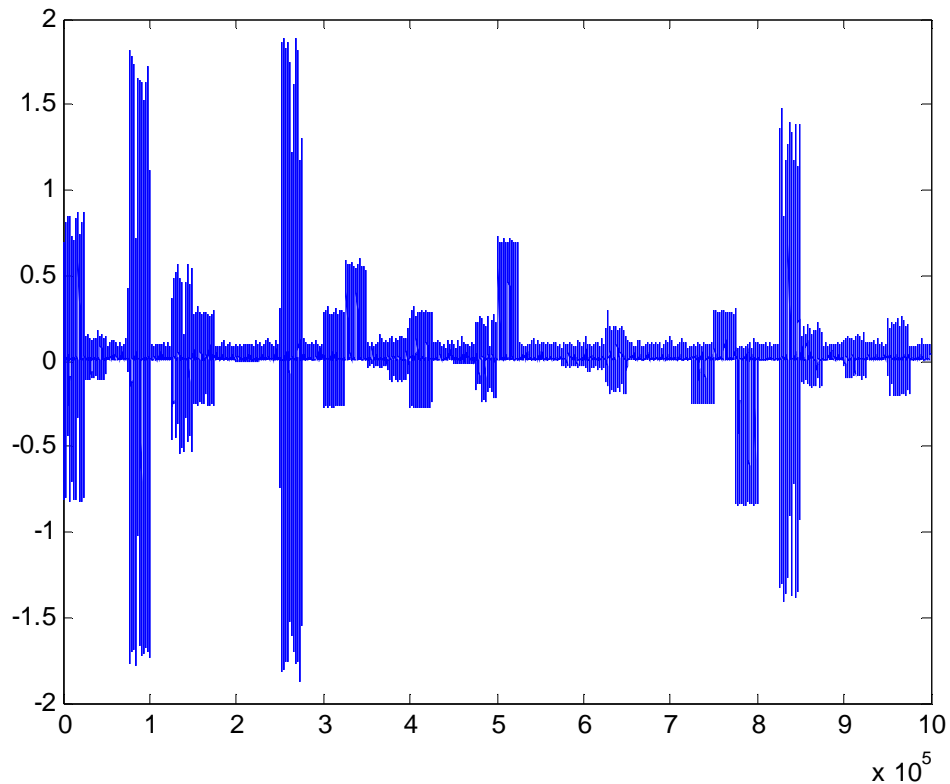


**Fig 6.11 Simulated radar base band data of a complete 360 degree scan containing multiple targets, clutter returns and noise background [x]**

This is the base band signal of one of the two channels. The clutter returns have high amplitudes and are decorrelated in time. There are four targets in the signal embedded in noise background and clutters. Now firstly the clutters are removed by using two techniques.

- Delay line cancellers.
- Adaptive Filtering technique (implemented from an IEEE paper) [5]

## 6.3 Stage 3

### Detection Process

Shown below is the output of delay line canceller algorithm.. But this technique is not efficient when the clutter is decorrelated or there is a Doppler shift in it.

In case when the clutter was not decorrelating in time the outputs of the DLC's and Adaptive Filter were not very much different. If the clutter is also decorrelated then the clutters may also pass through delay line cancellers as target. .But if we use adaptive filtering technique then this flaw is compensated in an efficient manner as shown in the figure below.

### Output of DLC

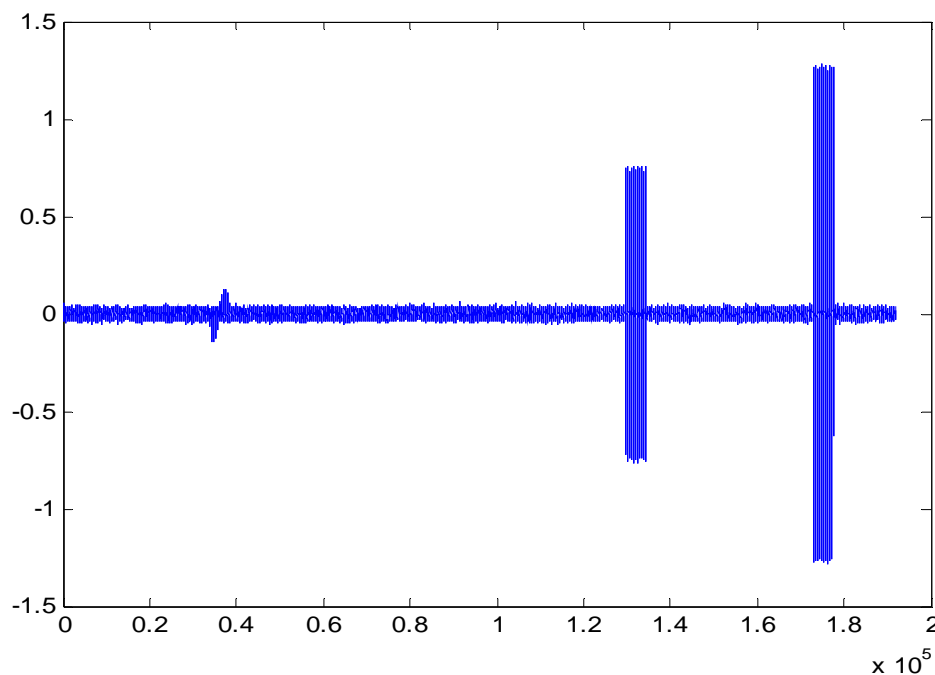


**Fig 6.12 Output of DLC when clutter was not decorrelating in time [x]**

## Output of Adaptive filter

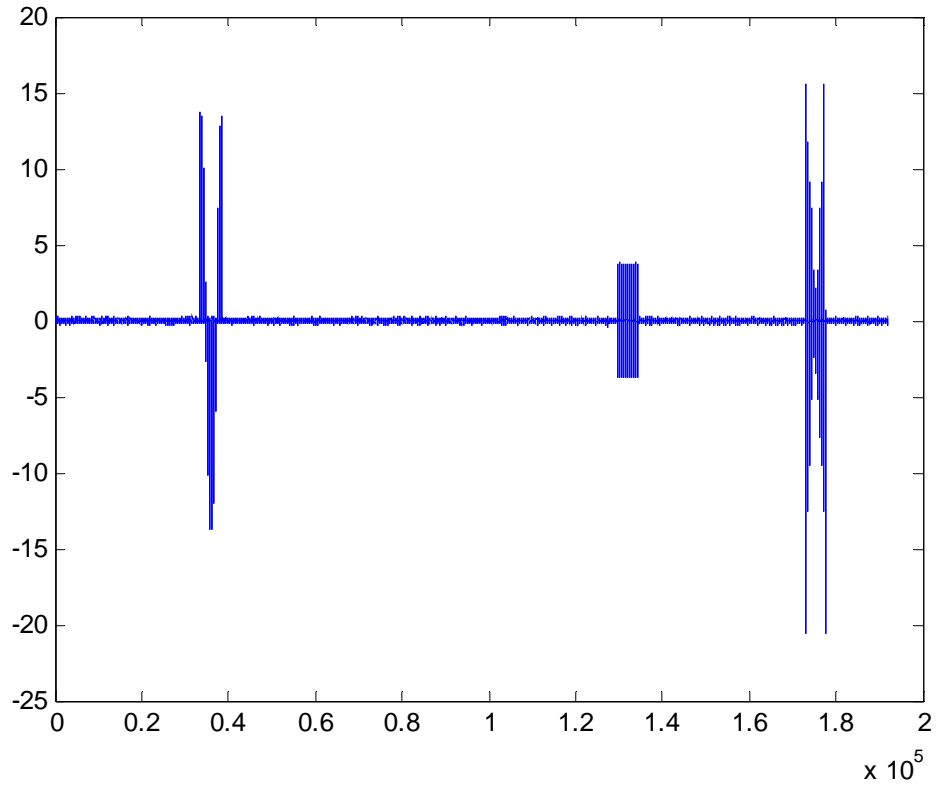


**Fig 6.13** Output of Adaptive Filter when clutter was not decorrelating in time [x]

But when the clutter was decorrelating the output of DLC was given by

### Output of DLC

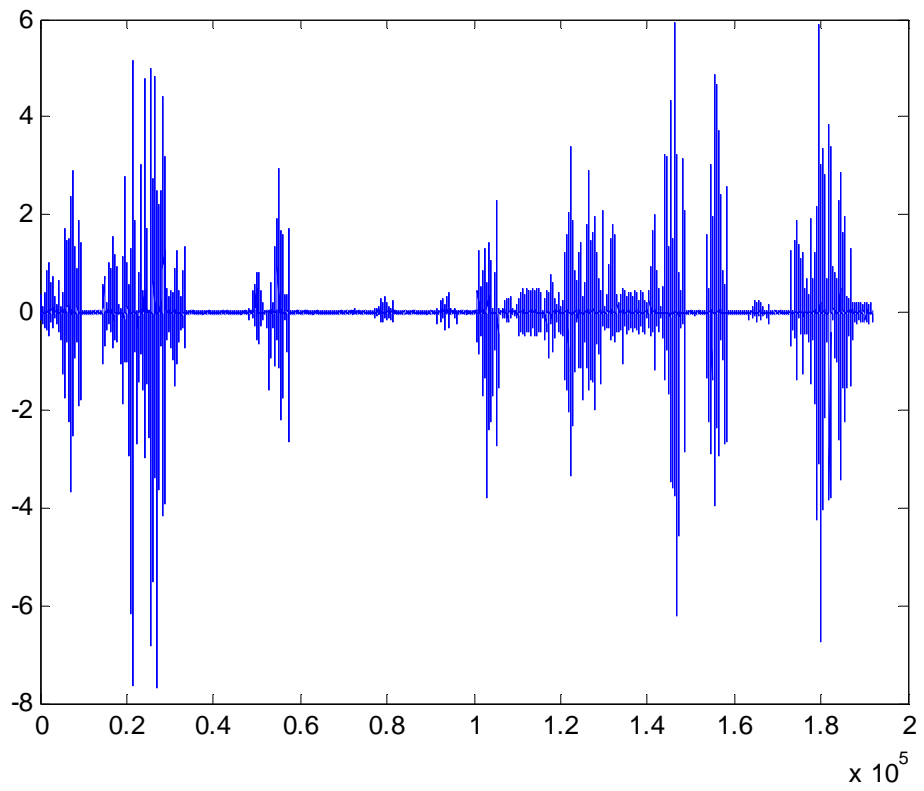


**Fig 6.14 Output of DLC when clutter was decorrelating in time [x]**



## Output of Adaptive Filter

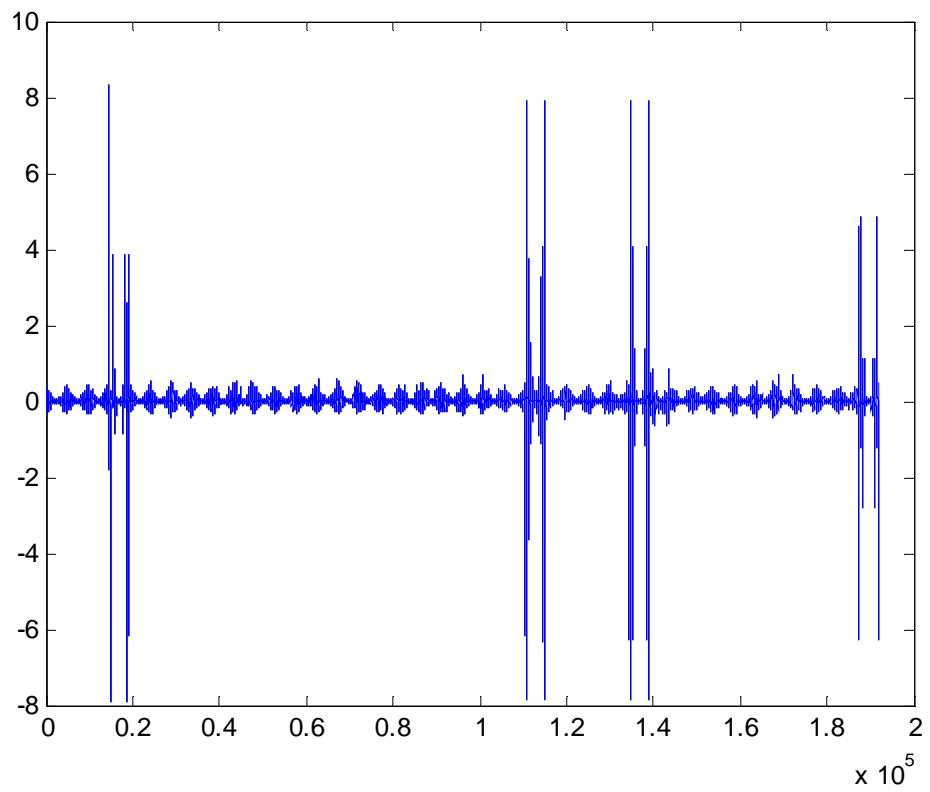


**Fig 6.15 Output of Adaptive Filter when clutter was decorrelating in time [x]**

## 6.4 Thresholding

An intelligent operator can sort out the targets manually from the clutter filtered output. But for the computer to perform this task, a threshold is required to be set, for target detection.

We have used different techniques for it which are as follows:

- Cell averaging CFAR
- Ordered statistical CFAR
- Maximum likelihood CFAR.(implemented from IEEE paper)

## 6.5 Cell averaging CA CFAR.

Signal level in a few bins on each side of the bin being tested for a target is averaged together. It is assumed that these bins contain only interference. The average value of the signal in these bins is multiplied with a constant and the result is threshold. Thus the probability of false alarm is established.

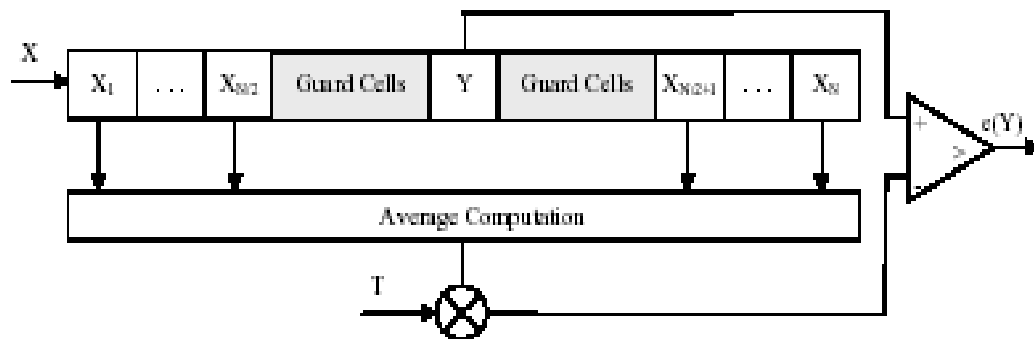


Fig 6.15 Block diagram of a CA-CFAR processor [6]

$$Y_{AC} = \begin{cases} \frac{1}{2}(S_L + S_R) \\ \max(S_L, S_R) \\ \min(S_L, S_R) \end{cases} \quad e(Y) = \begin{cases} 1, & \text{if } Y \geq T \times Y_{AC} \\ 0, & \text{if } Y < T \times Y_{AC} \end{cases}$$

Where  $S_l$  is left average,  $S_r$  is right average.

### 6.6 CA-SO-CFAR

If  $Y = \min(S_L, S_R)$  then CFAR is called Smallest Of Cell Averaging -CFAR. In Case of Our simulation the results of SO-CFAR with four targets is shown below

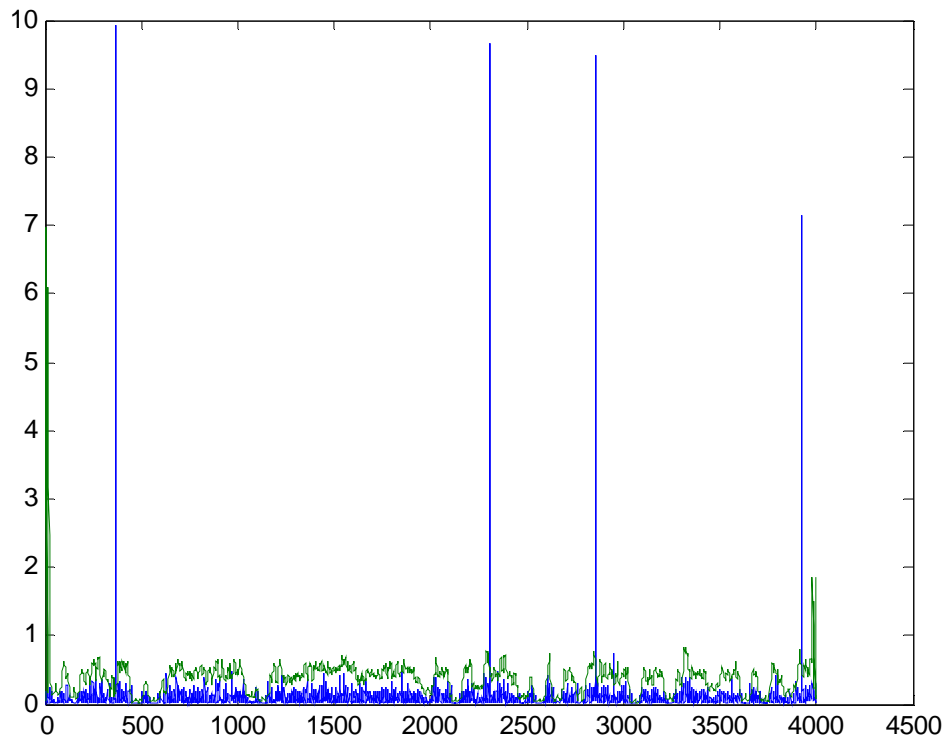


**Fig 6.16** Output after application of CA-SO-CFAR algorithm [x]

## 6.7 CA-GO-CFAR

If  $Y = \max(S_L, S_R)$  then CFAR is called Greatest Of CA-CFAR. In Case of Our simulation the results of GO-CFAR with four targets is shown below

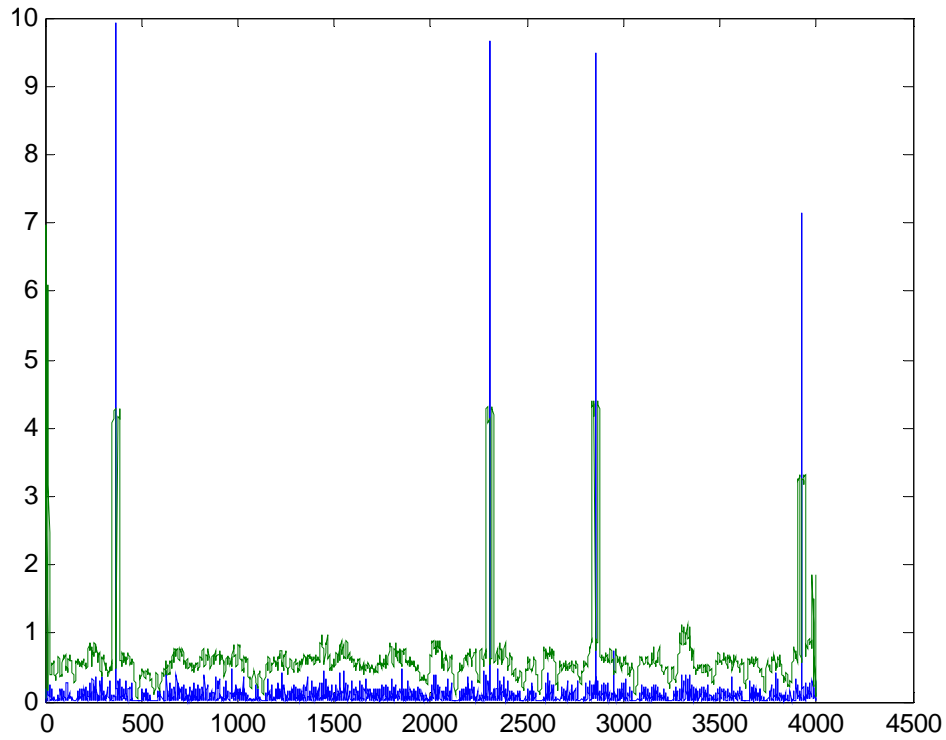


**Fig 6.17 Output after application of CA-GO-CFAR algorithm [x]**

### 6.8 CA-AVE-CFAR

If  $Y = \frac{1}{2}(S_L + S_R)$  then the CFAR is called Average of CA-CFAR. In Case of Our simulation the results of AVE-CFAR with four targets is shown below

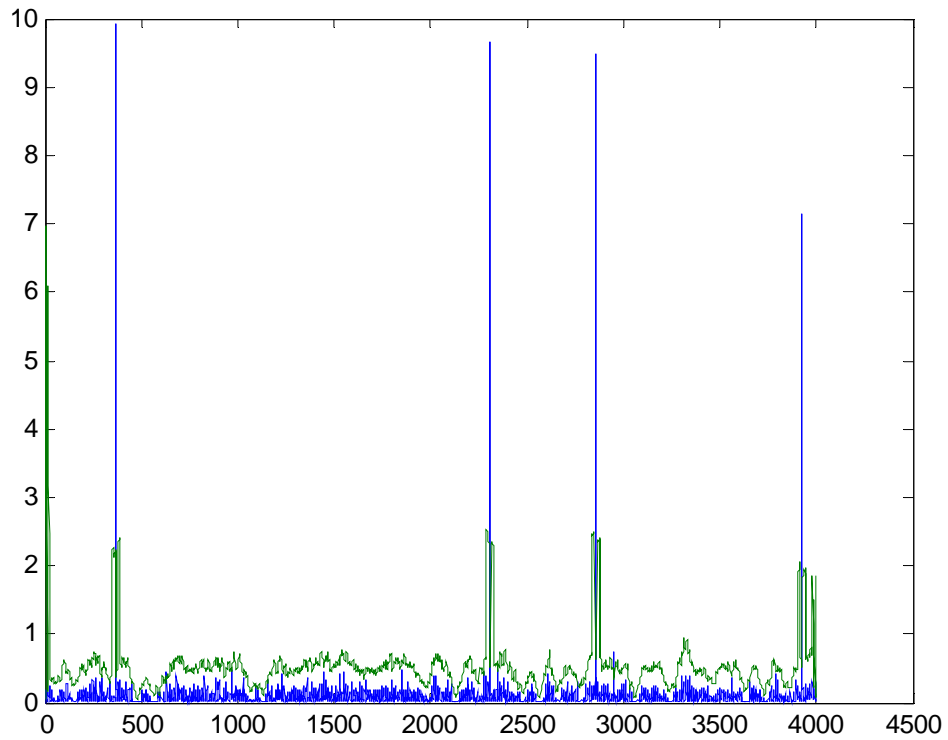


Fig 6.18 Output after application of CA-AVE-CFAR algorithm [x]

## 6.9 OS-CFAR

Applying CAGO-CFAR in the detection procedure brings several advantages in clutter transition areas. But the CA and CAGO-CFAR detection procedures behave very sensitively in multiple target situations and show pure performance.

The general idea of an ordered statistic is technically simple. To estimate the average noise and clutter power a single rank  $X(k)$  of the ordered statistic is used instead of the arithmetic mean. In this case a very few large amplitudes in the sliding window have a very small effect on the estimation result. OS-CFAR is robust in multiple target situations. The threshold is hardly influenced by a second or third target inside the window.

All amplitudes inside the sliding window are sorted according to increasing magnitude.

$$X_{(1)} \leq X_{(2)} \leq \dots \leq X_{(N)}$$
$$Z = X_{(k)}$$

The result of our simulation for the same four targets is

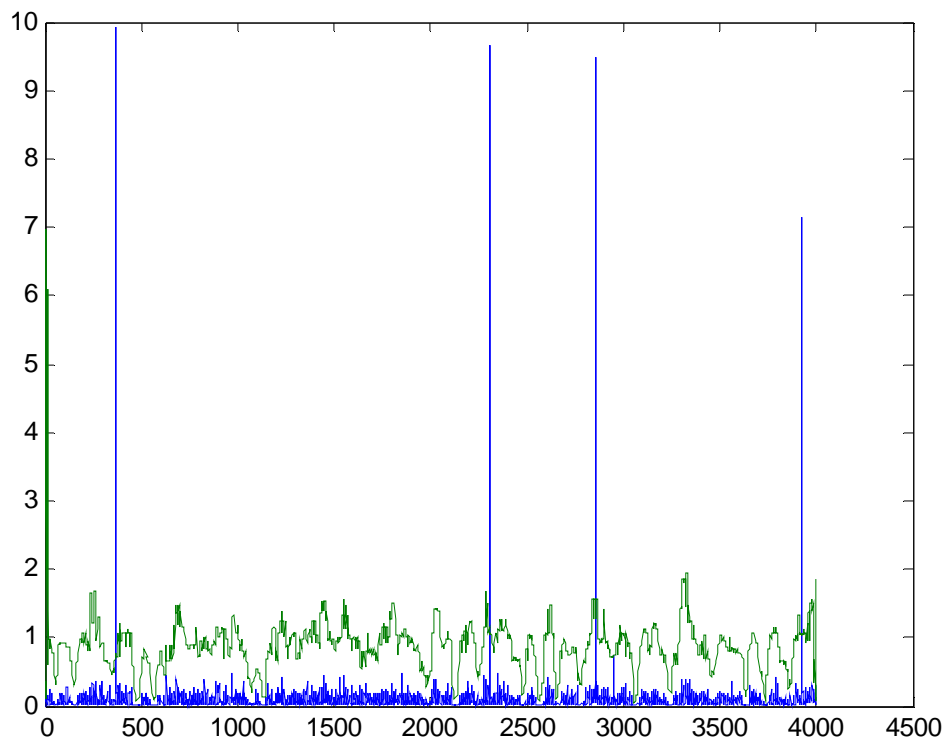


**Fig 6.19 Output after application of OS-CFAR algorithm [x]**

## 6.10 Maximum Likelihood Estimator -CFAR

If the background of the base band samples are described by Weibull distribution which is normally case for clutters at low grazing angle clutters and high resolution sea clutters then MLE-CFAR technique is optimum

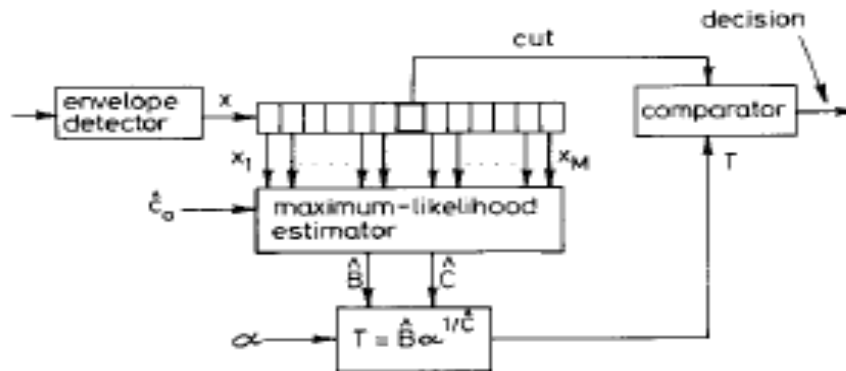


Fig 6.20 MLE-CFAR processor [4]

We arrange the cells of the sliding window in a array. We say it  $\hat{x}$ . From that array we estimate the values of the shape parameter  $\hat{C}$  and scale parameter  $\hat{B}$  of the samples under test which are assumed to be Weibull distributed.

$$\hat{x} = (x_1, x_2, \dots, x_M)^T$$

by solving iteratively for  $\hat{C}$  the equation

$$\frac{\sum_{j=1}^M x_j^{\hat{C}} \ln x_j}{\sum_{j=1}^M x_j^{\hat{C}}} - \frac{1}{\hat{C}} = \frac{1}{M} \sum_{j=1}^M \ln x_j$$

and using this  $\hat{C}$ , obtain  $\hat{B}$  from

$$\hat{B} = \left( \frac{1}{M} \sum_{j=1}^M x_j^{\hat{C}} \right)^{1/\hat{C}}$$

Threshold is calculated by following equation

$$T = \hat{B} \alpha^{1/\hat{C}}$$

Where  $\alpha$  is a constant depending upon the radar system specifications [4]

In case of our simulation the results were as described below

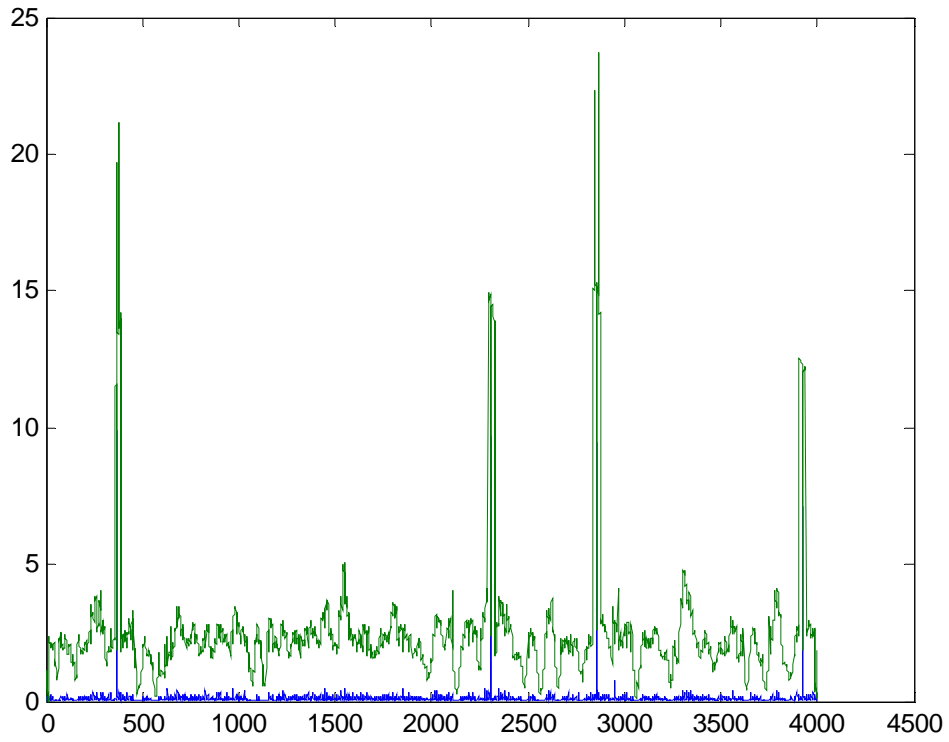


**Fig 6.21 Output after application of MLE-CFAR algorithm [x]**



## 6.11 Spectral Estimation

After the targets have been detected then their Doppler shifts have to be estimated. For this particular purpose several methods have been proposed. FFT which is traditionally used to estimate the frequency components of a signal performs quite poorly in case radar signals. This is so because the no. of samples on which FFT has to be applied are not in sufficient quantity which directly influence spectral resolution. Secondly the spectral leakages of FFT are very high.

In our case the output of FFT of combination of four targets is given below

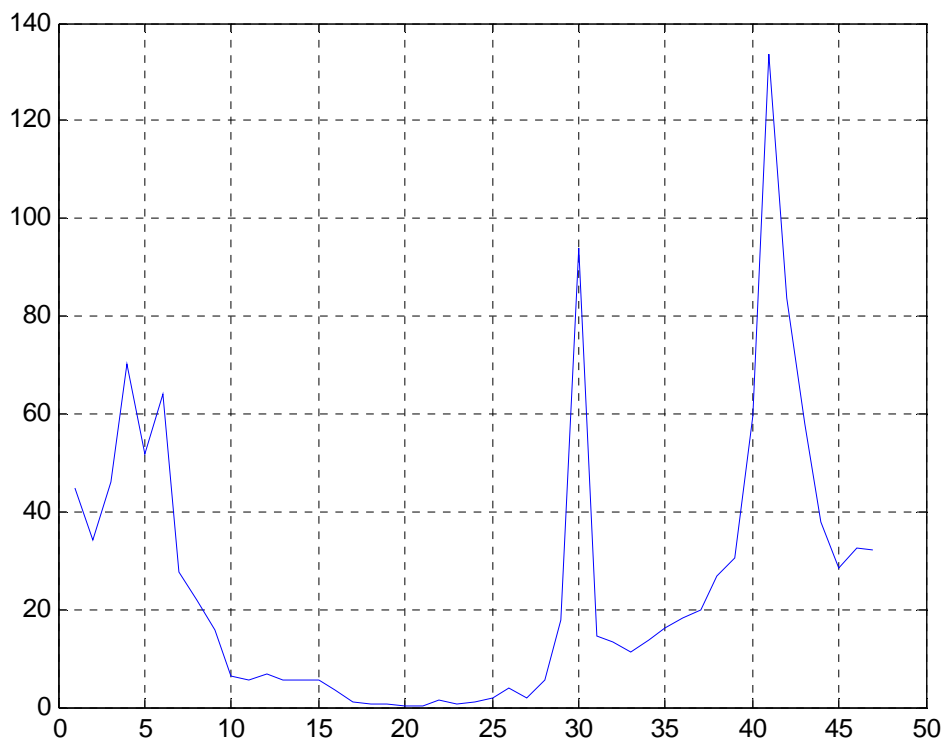


**Fig 6.22 Output of FFT of the four targets [x]**

We have tested a new idea to find spectral contents in which we implemented an IEEE paper stating “A NEW SPECTRUM ANALYSIS APPROACH USING AUTOCORRELATION TECHNIQUE AND MEM “[6]

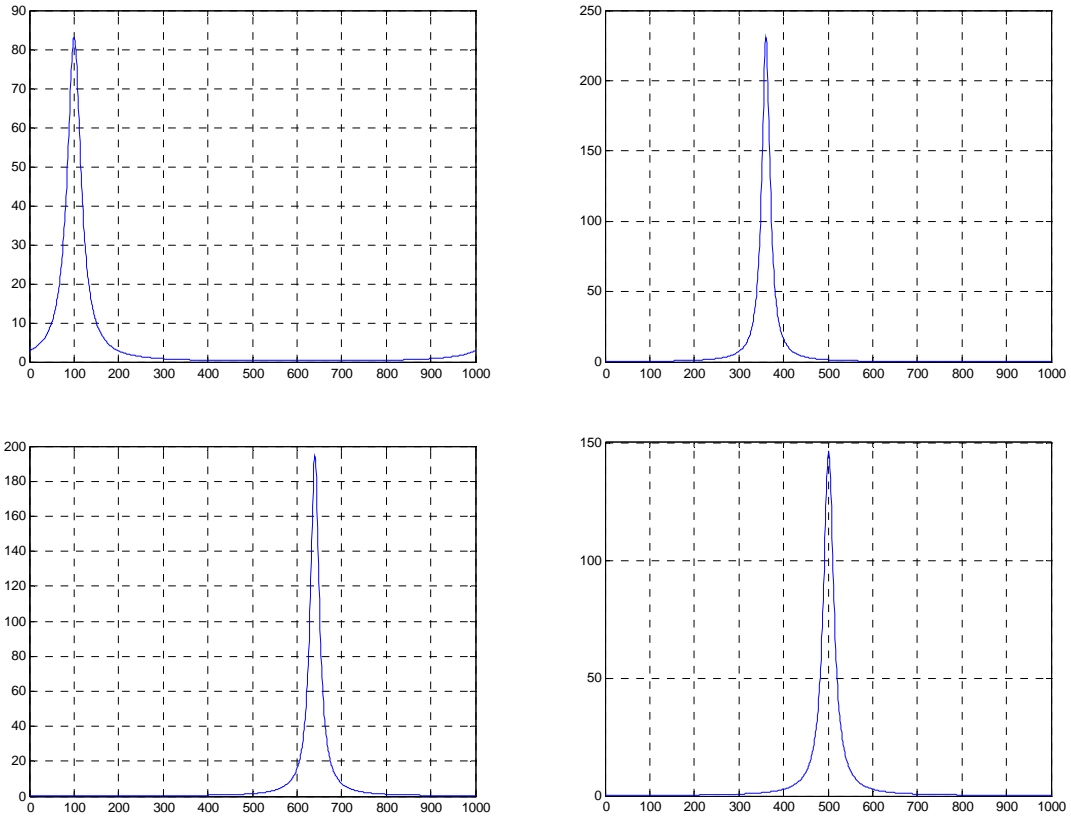


**Fig 6.23 Frequency of four targets clearly indicated by the Spectral Peaks of the output of the MEM [x]**

## 6.12 Tracking

The next stage of our Project was tracking. For this purpose, data of multiple scans was generated containing multiple targets. The data of each scans was processed and targets were detected. Then the processed data was fed to tracker. Two types of tracker were implemented, alpha-beta and alpha-beta-gamma tracker. PPI display was updated after every scan. Our simulation shows three targets.

**Plan Position Indicator (PPI) Display**

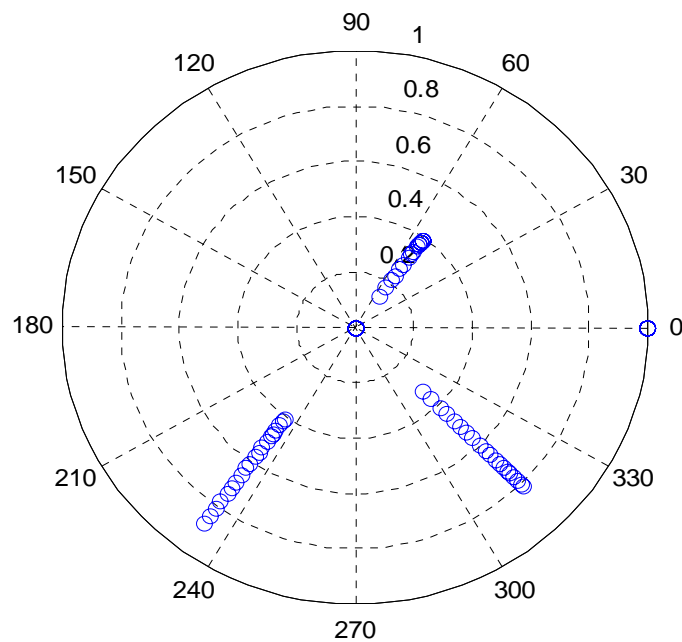


**Fig 6.24 PPI Display of three targets being tracked updated after each scan [x]**

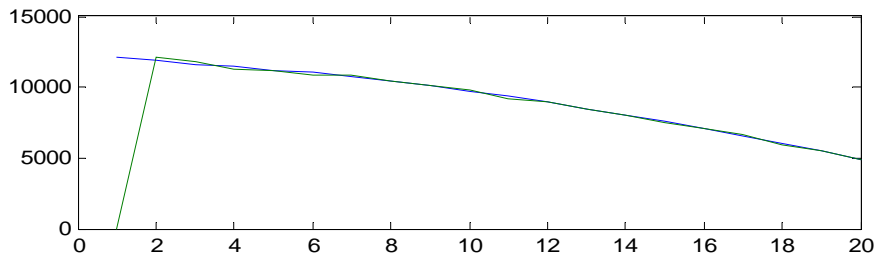
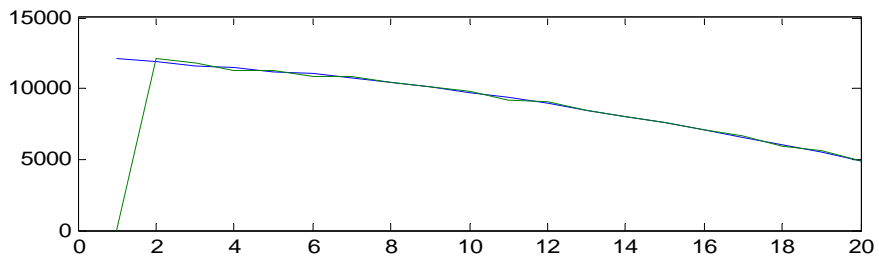


**Fig 6.25** Outputs alpha-beta and alpha-beta-gamma tracker for target no.1 [x]

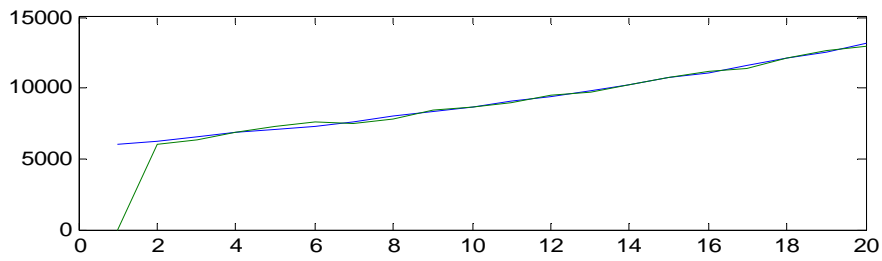
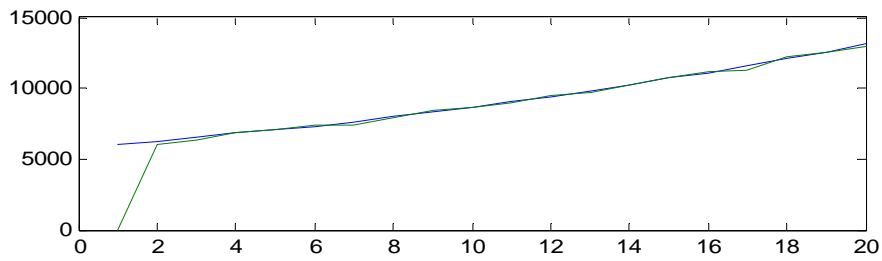


**Fig 6.26** Outputs alpha-beta and alpha-beta-gamma tracker for target no.2 [x]

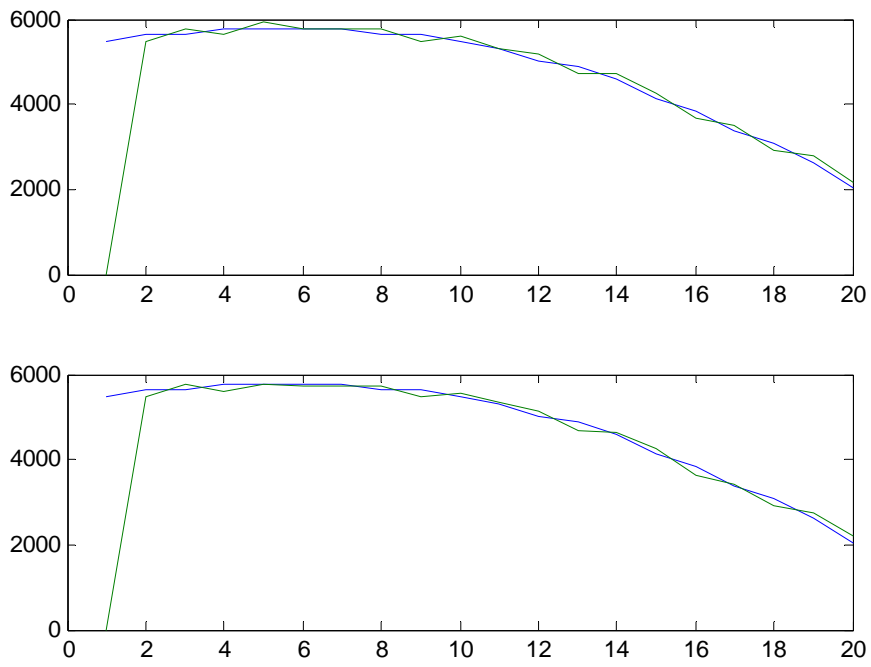


**Fig 6.27 Outputs alpha-beta and alpha-beta-gamma tracker for target no.3 [x]**

## 6.16 Stage 4

### Work on actual Radar Signal

In our final stage we tested the best indicated techniques on the original radar signal. The results are shown below.

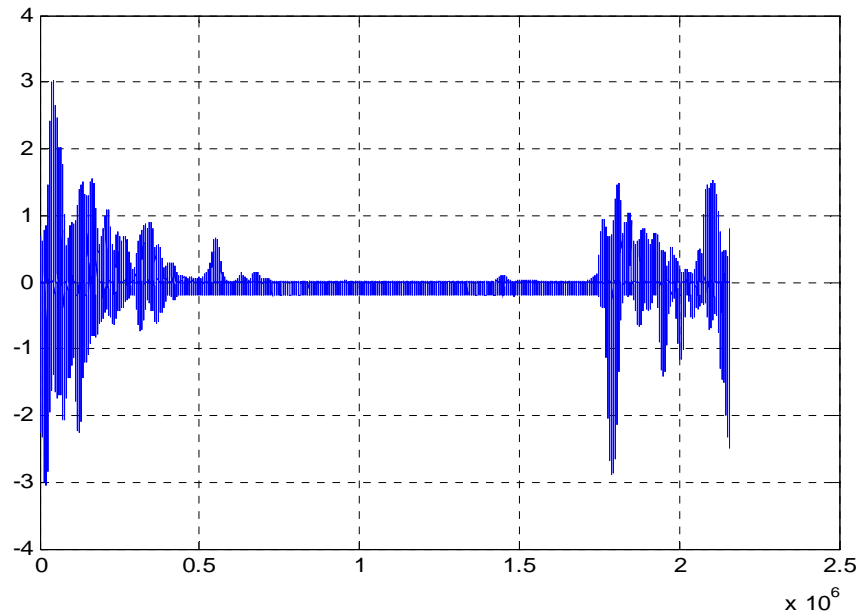


**Fig 6.28 Actual Radar Signal [x]**

### Clutter Filtered Output of Adaptive Filter

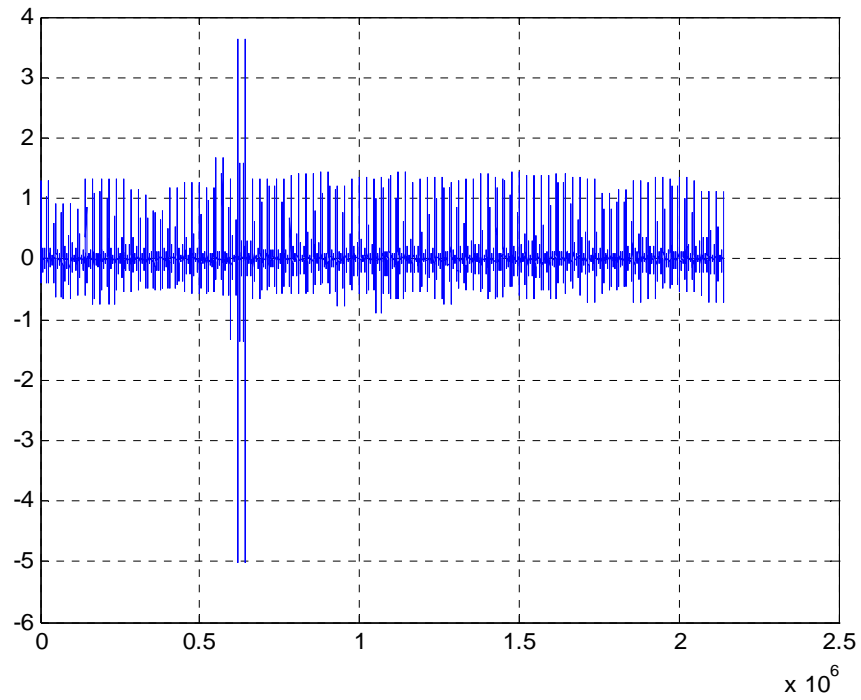


**Fig 6.29 Actual Radar Signal after adaptive clutter filtering [x]**

### Target Signal after OS-CFAR Thresholding

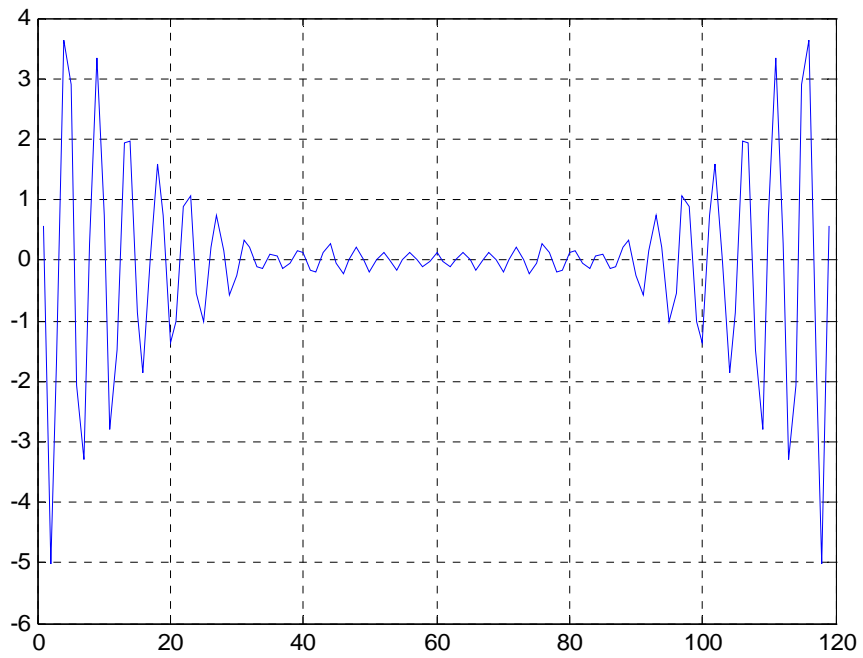
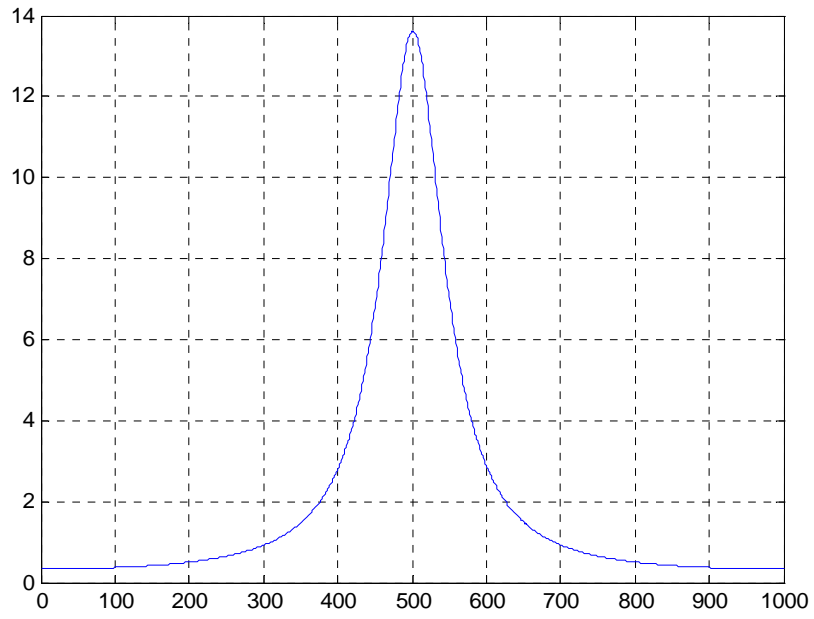


Fig 6.29 Threshold radar signal [x]



## Signal Frequency Spectrum Using MEM



**Fig 6.30 Spectral Estimate of the threshold signal [x]**

# Conclusion

The objective of processing of a radar signal is to detect target(s) in the presence of noise and clutter returns. Process of tracking follows the detection. The very presence of clutter and noise makes the whole job very demanding which are modeled as random process. The complexity of the scenario becomes of a great magnitude if we take into account the decorrelating clutter and noises of different distributions. Conventional techniques fail miserably in such a situation. We have tried to give a comparative analysis of techniques in use and several new algorithms described in different IEEE publications. In this regard we have implemented three IEEE papers in our comparative study. We simulated the detection and tracking process on a self generated radar signal in Matlab. The advantages and disadvantages of the techniques employed are analyzed at the end. Finally the best indicated algorithms are applied for the processing of actual radar signal.

# *Bibliography*

- [1] Skolnik, M, I, *Introduction to Radar Systems*, John Wiley & Sons, New York, 2001 Chapter 1, 2, 5 and 6
- [2] Edde, B., *Radar Systems*, John Wiley & Sons, New York, 2001 Chapter 1 and 6
- [3] Mahafza, B. R., *Introduction to Radar Analysis*, CRC Press, Boca Raton, FL, 1998 Chapter 3, 4, 6 and 9
- [4] *Maximum Likelihood CFAR for Weibull Background* IEEE Paper by N. Levanon and R. Ravid
- [5] Paul E. Rademacher and Benjamin A. Centril “*A Clutter Filtering and processing technique for EMI detection and angle measurement in Pulse Doppler radars*” *IEEE Transaction*
- [6] Hui S. K. and Lim Y. C. “*A New spectrum approach using autocorrelation technique and MEM*” *IEEE Trans.*
- [7] Stearns, S. D. and David, R. A., *Signal Processing Algorithms*, Prentice-Hall, Englewood Cliffs, NJ, 1988.
- [8] Stemson, G. W., *Introduction to Airborne Radar*, Hughes Aircraft Company, El Segundo, CA, 1983.
- [9] Brookner, E., *Tracking and Kalman Filtering Made Easy*, John Wiley & Sons, New York, 1998.
- [x] Matlab generated Output